THE URBAN HEAT ISLAND EFFECT IN DENSELY POPULATED URBAN AREAS AND ITS IMPLICATIONS ON ECO-CITY PLANNING: INVESTIGATION OF VERTICAL TEMPERATURE PROFILES IN DOWNTOWN VANCOUVER

by

Dana May

A project report submitted in partial fulfillment of the requirements for the degree of

BACHELOR OF TECHNOLOGY IN ENVIRONMENTAL ENGINEERING

in

SCHOOL OF CONSTRUCTION AND THE ENVIRONMENT

Submitted to:

Olga Petrov, PhD, Project Course Faculty, Program Head, Environmental Engineering

Fiona Lemon, MA, Project Course Faculty, Communications

Advisory Committee:

Olga Petrov, PhD, Project Course Faculty, Program Head, Environmental Engineering

Eric Saczuk, PhD, Faculty Instructor, Geomatics Engineering

BRITISH COLUMBIA INSTITUTE OF TECHNOLOGY

(Burnaby)

09/05, 2021

Abstract

The urban heat island (UHI) effect at the surface level of urban areas is influenced by the 3D characteristics of the local landscape, including vegetation cover and material types. However, further research is needed to understand the effect of urban features on local vertical atmospheric profiles within dense urban areas. Findings would assist with eco-cities design planning. This study collected vertical temperature data with Remotely Piloted Aircraft Systems at four sites within downtown Vancouver, chosen to represent varying levels of urbanization and surface coverage. Data was collected in the morning and afternoon in two seasons: summer and winter. Temperature profiles were compared against site characteristics including percentage vegetation and tree canopy coverage, percentage impervious surface coverage, building heights, and material types. A significant difference was noted between the four sites in the summer (up to 4°C), but not in the winter. In the summer, the most urbanized site with the lowest total vegetation (16%), highest impervious surface coverage (83%), and greatest number of tall buildings (6), had the warmest air temperatures in both the morning (17.84°C) and afternoon periods (21.30°C), though its surface temperature was cooler, likely due to shading. This warming effect persisted through to the highest measured altitudes. The least urbanized site (a park) with the highest total vegetation (49%) had consistently cooler air temperatures (morning: 16.78°C, afternoon: 18.74°C). Two sites located near the ocean did not behave as expected: one had high afternoon air temperatures (20.81-21.21°C) despite proximity to large heat mitigation features, while the other had the lowest afternoon air temperatures (17.92°C) despite low percent vegetation (21%) and high imperviousness (59%). Air temperatures at these sites were likely influenced by advection forces due to the predominant direction of coastal land-sea breezes. In the winter, temperature profiles showed less variation, under 1°C, and exhibited similar profile changes with altitude, suggesting that microscale variations in the vertical UHI are more prevalent in the summer. Additional research on vertical temperature profiles in a variety of urban areas would be beneficial to better understand the impact of urban features on local atmospheric heat. Vancouver and the region have several strategic frameworks addressing urban heat and climate change, however these would benefit from greater emphasis on green infrastructure and high albedo building materials.

Acknowledgements

First, I would like to acknowledge my two advisors, Olga Petrov and Eric Saczuk, for helping to make this project a reality. Their support and guidance over the course of this endeavor were invaluable and a source of inspiration. Eric's hard work and commitment to finding and organizing the resources needed for such a complex undertaking as launching multiple drones simultaneously across the busy downtown Vancouver core was a wonderful help. Olga was a tireless source of encouragement and expertise, helping to guide me through the project steps and providing valuable insight into study design and interpretation of results.

Special thanks as well to Kyle Howe from Metro Vancouver for always being willing to answer my questions, provide resources, and lend an eye to my results. Additionally, I would like to thank Rodrigo Mora for helping spark the idea for this study and providing assistance with equipment and materials. The opportunity to take part in his pilot study on the BCIT campus enabled this whole process to take off, and allowed me to establish connections with some of the other key people that made this project possible.

Lastly, but certainly not least, thanks to all of my classmates and friends who lent their time and assistance to help me with collecting and recording observations during test days. Specifically, Emily Lai, Peter Quan, Sarah Richardson, Sean Mak, and my wonderful partner, Eric Ringheim. Not only for lending your physical assistance, but also for always supporting me and helping to push me forward.

Table of Contents

List of Tables

List of Figures

List of Acronyms

ABL – Atmospheric Boundary Layer

ISL – Inertial Sublayer

RPAS – Remotely Piloted Aircraft System

RSL – Roughness Surface Layer

SVF – Sky View Factor

UAV – Unmanned Aerial Vehicle

UBL – Urban Boundary Layer

UCL – Urban Canopy Layer

UHI – Urban Heat Island

1.0 Introduction and Background

As the world struggles with climate change and rising temperatures, the effect of urban landscapes on local temperatures is becoming a phenomenon of public concern. Most city dwellers have experienced the discomfort of travelling on hot, dry asphalt streets and the challenge of falling asleep at night in the muggy heat at the peak of summer. And those same city residents may have looked for a reprieve from the summer heat in their shady neighbourhood park.

While these experiences are merely anecdotal, this phenomenon has a technical name: the Urban Heat Island (UHI). The UHI is defined as the existence of recognizably warmer temperatures within urban areas compared to those in rural areas (US Environmental Protection Agency [EPA], 2008; Health Canada, 2009). Urbanization has a significant effect on the surrounding atmosphere and is a driver of climate change through processes such as land degradation and deforestation, high proportions of heat-retaining materials, and increased per capita emissions of greenhouse gases (Intergovernmental Panel on Climate Change [IPCC], 2019). Heat waves are known to be more intense within cities, and have been correlated with adverse health impacts, including increased mortality, especially for vulnerable populations such as the chronically ill, elderly, and young children (IPCC, 2019; Giguere, 2012). Heat also plays a key role in the chemistry of air pollution and photochemical smog formation (Giguere, 2012; Lesnikowski, 2014; EPA, 2008). At present, population distributions are shifting towards cities, and it is expected that 70% of the global population will live in cities by 2050 (IPCC, 2019). With so much of the population dwelling in urban regions, it is more important than ever for municipalities to adapt to rising temperatures through the use of heat mitigating urban and building design strategies.

Vancouver has typically enjoyed a mild and temperate climate, and its urban design policy has historically focused on features that take advantage of periods of sunlight or on protection from frequent rain (Lesnikowski, 2014). Because of this historically temperate climate and the accompanying design policy, Vancouver may be more vulnerable to the negative impacts of increasing temperatures. In particular, the frequency of annual heat days – where the temperature exceeds 30°C – is expected to rise from two days up to 14 days annually by 2050, and has been noted as a concern in Metro Vancouver's Climate Projections (2016). Vancouver is thus a prime candidate for UHI research. In fact, the region has expressed an interest in better understanding its urban atmospheric heat profile and associated weaknesses. Such knowledge would allow Vancouver to shift its urban design policy towards better addressing rising temperatures.

1.1 Research Problem Statement

With the aforementioned issues in mind, a detailed understanding of the urban atmosphere and its influence on the UHI is needed. Previous research on the UHI has been fairly extensive, but investigations into the impact of the three-dimensional urban landscape on heat creation are more recent. Research specifically into the vertical structure of urban heat islands, however, is limited. Previous attempts to look at vertical temperature profiles have been based mostly on distance methods like aircraft mounted sensors or satellite imaging, which can require atmospheric interference corrections or have low resolutions (Voogt, 2017). Other attempts have used methods such as radiosondes or sensors affixed to structures, all of which come with limitations (Lokoshchenko et al, 2016; Voogt, 2017). Remotely Piloted Aircraft Systems (RPAS) present a new opportunity to explore the vertical microstructure of the UHI in dense urban areas with an improved level of flexibility and precision.

This research paper investigates whether urban characteristics and morphological features have an impact on the vertical temperature profiles and consequently on the UHI effect within the dense urban landscape of downtown Vancouver. Characteristics and morphological features considered include the urban canyon effect and 3D building structure, tree canopy coverage, material albedos, impervious surfaces, and vegetative features like green roofs. The objectives of this project are (1) to measure, analyze, and compare the vertical temperature profiles of four sites around downtown Vancouver with RPAS; (2) to assess whether the morphological features and characteristics of each site have any impact on the vertical temperature profiles; (3) to consider temperature profiles at each site in two separate seasons to assess seasonal variation; and (4) to consider the data and discuss results within the context of eco-city strategies, and apply the information gained to the City's and the Region's future heat mitigation strategies. Specifically, the City of Vancouver's Greenest City Action Plan (City of Vancouver, 2015), Vancouver's Urban Forest Strategy (City of Vancouver and Vancouver Park Board, 2018), and Metro Vancouver's Climate 2050 Framework (Metro Vancouver, 2019).

2.0 Literature Review

The following section reviews the available literature related to the urban atmosphere and urban heat island. First, the Urban Boundary Layer and the atmospheric processes within it as they are presently understood are explained. Next, the current literature around the UHI is discussed, beginning with an overview of known causes and mitigation strategies, and followed by a more detailed review of research into the role of urban morphology and 3D structure on the development and presentation of the UHI. Finally, studies that have investigated the vertical structure of the UHI are presented, including those addressing the role of RPAS in data collection.

2.1 The Urban Boundary Layer

The complex shape, structure, and thermal properties of metropolitan areas have a profound effect on the atmospheric conditions both above cities and within the local microclimates of individual neighborhoods (Barlow, 2014). Normally, the atmospheric boundary layer (ABL) – the layer of the atmosphere nearest to the earth and which extends to approximately 0.8 to 1 kilometers in height – is characterized by a predictable diurnal cycle. During the day, convective thermal mixing is triggered within the ABL by radiative solar heating of the surface. At night, radiative cooling of the surface occurs to form a stable cool layer with supressed mixing near the ground (Zenman, 2012). This cycle has been extensively studied and is well understood as it occurs above natural, homogenous terrain such as that found in rural or natural areas (Zenman, 2012). This is not the case for dense urban areas, however, where the complexity of surfaces and general lack of vegetation leads to considerably rougher, drier surface features, and a subsequent alteration in the known structure of the ABL.

In urban areas, the ABL is redefined as the urban boundary layer (UBL). The UBL is one of the least understood atmospheric regions, and thus is an area of considerable study in recent literature (for review, see Barlow, 2014). The UBL can be divided into several distinct sublayers. At a high level, the UBL consists of the roughness surface layer (RSL), and the inertial sublayer (ISL). The RSL is the layer of air extending from the surface to about 2-5 times the average building height and is dominated by spatially variable turbulent flow[1]. The ISL, on the other hand, lies above the RSL and is a region of relatively homogeneous flow (Barlow, 2014; Zenman, 2012). At present, there is some debate about whether the ISL is always present above cities (Barlow, 2014). Below the ISL, the RSL can be further broken down into two sub-layers: At the lowest level, the Urban Canopy Layer (UCL) occupies the space between the ground and the average height of the surrounding buildings. Above the average building height, a nameless, strong shear layer exists which is predominated by high winds and elevated turbulence and mixing (Zenman, 2012).

The UCL is characterized by spatially variable microclimates that are highly dependent on the surrounding buildings and local features of each area – a quality that makes the UCL difficult to draw general conclusions about (Barlow, 2014; Zenman, 2012). Within the UCL, local turbulence has different characteristics from those seen in other layers. Local flow patterns are uniquely influenced by the changing surface roughness as air moves through varying suburban, park, and urban areas. Additionally, flow patterns are influenced by the diverse thermal properties of urban materials within these regions (Barlow, 2014). These characteristics all play into the urban surface energy balance which in turn drives the atmospheric processes above

[1] Turbulence is defined as the agitation or unsteady movement of a fluid such as air or water, including chaotic changes in pressure and velocity and mixing between flow lines

(Barlow, 2014). Ultimately, each unique local neighborhood microclimate within the UCL starts off in equilibrium with the surface beneath it. But as altitude increases, these small climate zones begin to mix, up through a transitional blending layer that eventually extends to the top of the RSL. At the top of the RSL and beyond, relative consistency of flow is achieved in the ISL (Barlow, 2014). Figure 1 provides a simplified visual representation of this region.

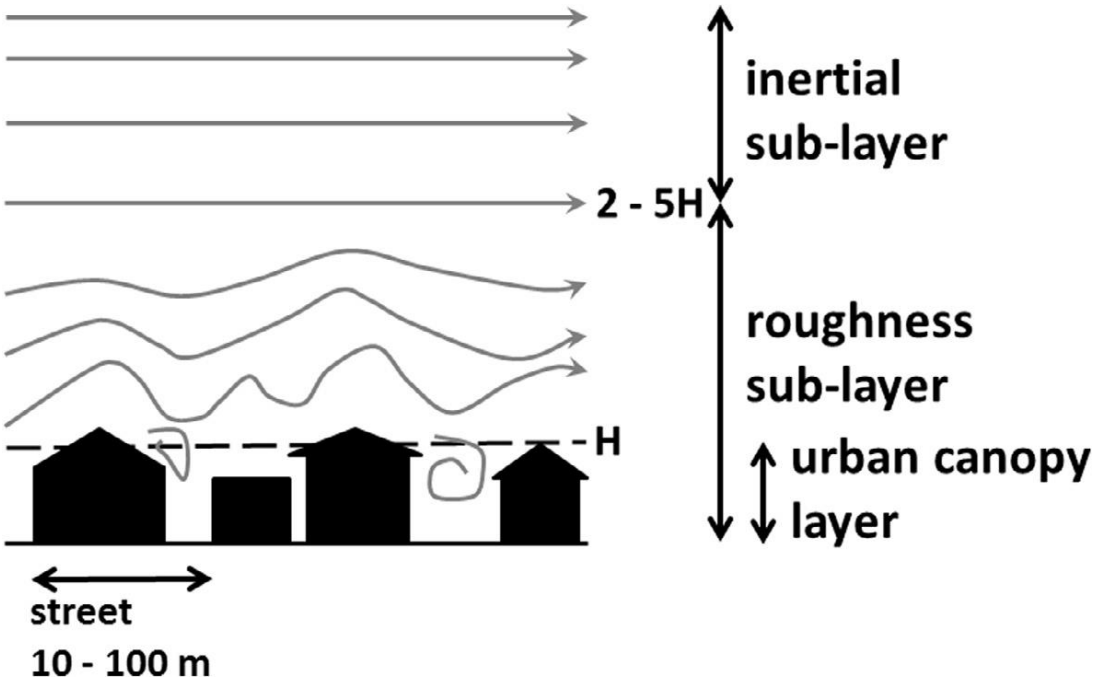

Figure 1: Schematic representation of the urban boundary layer and sublayers, with streamlines shown in grey (reproduced from Barlow, 2014).

Despite the challenges encountered in characterizing it, the UCL is the space within which humans spend most of their time, and thus is a microclimate that we cannot ignore. Efforts to model and better understand the unique characteristics that define the different regions of the UBL are extensive (Adkins, 2020; Barlow, 2014; Wang et al., 2013). Continued research into understanding the influence that cities have on the presentation and structure of the UBL are warranted for many reasons. One important reason is that the behaviour of the UBL and the UHI both play a role in pollution formation and dispersion, and thus on human health and comfort (Adkins, 2020; EPA, 2008; Giguere, 2012; Masic, 2019; Salata et al., 2017; Zenman, 2012). Pollution accumulates in cities from point sources such as buildings or backyard firepits, as well as non-point sources such as vehicle exhausts. Urban air quality is then made worse in high temperatures when these pollutants mix in the presence of heat and light to produce photochemical smog, a toxic and unsightly mixture of ground level ozone and other

pollutants. Since temperatures are generally hotter in urban areas because of the UHI, the UHI effect ultimately contributes to poor air quality. Moreover, the behaviour of air flow within the UCL is important because it influences the movement of pollutants like ground level ozone. Complex flow patterns around buildings within the UCL and their impact on plume lift and mixing are bound to affect the way ground level pollutant emissions accumulate or are dispersed at local scales (Zenman, 2012). An improved understanding of the vertical atmospheric profile within and above urban neighborhoods would contribute meaningful information to the impact that urban design parameters have on how we manage air pollution. An understanding of the triggers for air pollution events will help us to better manage and prevent the increases in morbidity and mortality associated with periods of poor air quality and high heat (EPA, 2008; Masic et al., 2019; Zenman, 2012).

2.2 Urban Heat Islands: Overview and Causes

The urban heat island (UHI) is an atmospheric phenomenon that manifests as a region of warmer temperatures within and over urban areas compared to the temperature of surrounding rural areas (EPA, 2008; Health Canada, 2009). Health Canada (2009) notes that this effect usually occurs over large metropolitan areas where built surfaces tend to absorb large quantities of solar radiation during the day. However, the EPA (2008) states that the effect has been noted even over smaller cities and towns, though the size of the temperature effect declines as the urban area decreases in size. UHIs can be classified into surface urban heat islands and atmospheric urban heat islands, with each denoting the area where the change in temperature is observed (EPA, 2008; Giguere, 2012). The existence of built-up urban features has been observed to cause temperatures that are 2°C to 12°C higher than non-urban areas (EPA, 2008; Giguere, 2012; Health Canada, 2009), with the highest temperature differences occurring at night (EPA, 2008).

The UHI phenomenon has been documented as far back as the 19th century, when Luke Howard noted a 4°C temperature difference between London and the surrounding countryside (Stone, 2012, as cited in Lesnikowski, 2014). Since then, a large number of studies have observed and attempted to understand the UHI effect around the globe. Hence, the behaviour, features, and causes of the UHI have been discussed in a wide variety of literature sources (e.g., Arnfield, 2003, as cited in Barlow, 2014; Zenman, 2012), including provincial (Giguere, 2012) and national guidelines (Health Canada, 2009; EPA, 2008). According to Giguere (2012), the main contributors to UHIs are the low vegetative cover, high proportion of impermeable surfaces, urban morphology, greenhouse gas emissions, anthropogenic heat, and thermal properties of surface materials.

A major side-effect of urbanization is the loss of vegetation, especially tree cover. As vegetation is removed during urbanization, it is usually replaced by impervious materials like

asphalt, concrete, and buildings. This loss of vegetation decreases ground shading and reduces cooling of the air by evapotranspiration (EPA, 2008; Zenman, 2012; Lesnikowski, 2014). Furthermore, when vegetation is replaced with impervious materials, there is an increase in runoff and a reduced penetration of rain and stormwater into the ground and soil. Normally, heat in the air is dissipated by the evaporation of moisture from the ground when temperatures increase. However, when impervious materials replace the natural ground surface this evaporative cooling process is disrupted (Giguere, 2012; Lesnikowski, 2014).

To combat the UHI, some regions have implemented urban greening policies aimed at boosting the proportion of vegetation within urban areas. Strategies include the encouragement of green infrastructure such as green roofs and walls on buildings. Other approaches include municipal tree planting strategies (Metro Vancouver, 2019; City of Vancouver and Vancouver Park Board, 2018), and discouraging the removal of trees on private property through the requirement of permits (Lesnikowski, 2014). Green roofs have been demonstrated to be consistently cooler than other roof types in summer, even light-colored roofs (for review, see EPA, 2008). Green roofs also have a number of benefits in addition to cooling, such as providing space for urban agriculture, extending the life of the roof, assisting with stormwater collection, and improving air quality (EPA, 2008; Giguere, 2012). The existence of urban parks instead of buildings can also decrease the surrounding air temperature by up to 6°C (Giguere, 2012). In fact, the existence of a vegetated “green island” within an urban area has been shown to provide cooling effects that may reach up to 40m or more beyond its edges, depending on wind and the size of the island. In addition to greening strategies, municipalities are also addressing impermeability issues. Rain gardens, infiltration trenches, natural retention ponds, and constructed wetlands are all useful tools for improving permeability. These approaches add vegetation as well as helping to manage stormwater runoff and flooding. Other strategies used to address rising impermeability include encouraging the use of pervious surfaces like interlocking paving stones or gravel, as well as soil filled, structurally sound grid systems which allow root and water infiltration (Giguere, 2012).

The urban environment is a complex, three-dimensional landscape characterized by buildings of various sizes, heights, and spacing. Urban morphology is the umbrella term which refers to these 3D structural characteristics, and includes concepts such as urban canyons and sky view factor (SVF; Giguere, 2012). Urban canyons are the narrow spaces in between tall buildings, while SVF is a measure of the amount of sky that is visible from a point on the ground surface (EPA, 2008; Giguere, 2012: Zenman, 2012). Other key concepts describe the different heights and sizes of those buildings, which can be expressed as average building height, or building height to length ratio (Zenman, 2012). These features play into the UHI effect in various ways, but primarily by trapping heat, or impacting the amount of solar radiation that is

able to reach the ground surface. Furthermore, morphological features influence temperatures by interacting with the flow of air and wind through neighborhoods.

The thermal properties of common urban materials also play a role in the formation of UHIs. Thermal properties include albedo, emissivity, and heat capacity. Albedo is a ratio indicating the proportion of solar radiation received by an object that is reflected[2] back from the surface rather than absorbed (Giguere, 2012; Zenman, 2012). A low albedo indicates that most of the solar energy received is absorbed[3], causing the object to heat up and by releasing that energy warm the surrounding area. Generally, darker coloured materials have lower albedos. Lesnikowski (2014) identified the abundance of dark, steeply sloped roofs on single family homes in Vancouver as a common problem in the city's many historic neighbourhoods and a likely contributor to UHI formation. Common building materials that have low albedo include asphalt (albedo: 5-20%), dark corrugated roof shingles (albedo: 10-16%), and dark colored tiles (albedo: 10-13%). In contrast, green areas have albedos ranging from 25-35% for low ground vegetation like grass, and 15-18% for trees (EPA, 1992, as cited in Zenman, 2012). Vegetation also converts much of the solar radiation that it absorbs into energy for growth and food via photosynthesis, rather than storing and emitting it to the surrounding air as heat.

Thermal emissivity, on the other hand, is a measure of a material's ability to release heat back to its environment (EPA, 2008; Zenman, 2012). Emissivity is dependent on a material's finish and on the temperature of the surroundings, which influence the rate of energy release. High emissivity materials hold onto heat longer and may increase the heating load of a building, or increase the heat of the nearby environment (Akbari & Konopacki, 1998). Some examples of typical emissivity values for urban materials include red brick (emissivity: 90%), polished aluminum (emissivity: 10%), and white paint (emissivity: 90%; Giguere, 2012). Both emissivity and albedo are properties that are closely related to a material's heat capacity, defined as the amount of heat required to raise a given mass of material by 1°C (Engineering Toolbox, 2003). Generally, materials found in cities have a higher heat capacity than natural materials such as soil or sand. This results in downtown metropolitan areas that can absorb and store double the heat that their rural surroundings would during a typical day (EPA, 2008). The interplay of these thermal properties in urban environments creates a complex interaction of incoming and outgoing solar radiation, which is stored or released back to the surrounding air in varying rates and amounts throughout the day and night.

2.3 The Role of 3D Structure and Urban Morphology

The impact of 3D urban morphology on air temperature in cities has been studied by a number of researchers in recent years (eg. Gage & Cooper, 2017; Jin et al., 2018; Tian et al.,

[2] Reflection is defined as the return of light, heat, or sound from a surface that it comes in contact with
[3] Absorption is defined as the integration of energy, a material or a substance into another material

2019). A consensus exists in the literature that the existence of vegetative features – specifically trees – is negatively correlated with temperature (Gage & Cooper, 2017; Jin et al., 2018; Lesnikowski, 2014; Tian et al., 2019; Yu et al., 2020), though the specific vegetative parameters studied varies. Gage & Cooper (2017) used LiDAR (Light Detection and Ranging), a remote sensing method, to perform hexagonal cluster analysis of land cover patterns in Colorado and found that tree canopy height played a role in land surface temperatures. Specifically, the authors noted that temperatures were higher in clusters where mean building height exceeded mean tree height, and cooler where trees were on average taller than surrounding buildings. Tian et al. (2019) noted that the ratio of the volume of vegetation to building volume played a significant role in urban temperatures in Beijing, but only in predominantly low-rise neighborhoods. In high-rise neighbourhoods, vegetation volume was less important than the orientation of buildings to solar radiation, measured as the ratio of east-west (E-W) to north-south (N-S) building length. Both of these studies support the importance of tall, mature trees for the shading properties they provide, a view maintained widely in the literature (Giguere, 2012; EPA, 2008; Lesnikowski, 2014; Zenman, 2012).

Building orientation and shape has been flagged as a major contributor to microclimatic temperature variation in cities. The orientation of buildings in relation to solar radiation as well as prevailing wind directions was noted to play a role in temperature of the surrounding air by Lesnikowski (2014), and Tian et al (2019). Urban morphology features within the UCL such as urban canyons and related SVF are also key players in neighborhood microclimates (Giguere, 2012; Zenman, 2012). Generally, deep urban canyons found in denser, high-rise dominated landscapes also have low SVF, meaning that less solar radiation can reach the ground surface. This was correlated with lower temperatures during the day, likely because of the shading provided by tall buildings (Jin et al., 2018; Tian et al., 2019). However, these same high-rise, low SVF neighborhoods also had comparably higher temperatures during the night (Jin et al., 2018; Tian et al., 2019). In urban canyons, solar radiation that does find its way between buildings is reflected back and forth, often being absorbed, released, and then reabsorbed by building materials within the canyon. Anthropogenic heat emanating from buildings due to energy consumption may also add additional heat to the landscape (EPA, 2008; Giguere, 2012; Jin et al., 2018). All of these factors result in heat taking longer to escape urban canyon regions at night, as reflected in the observed higher night time temperatures. In contrast, neighborhoods with shorter buildings and greater SVF, despite getting hotter during the day, had more effective surface radiative cooling from urban materials and thus cooled off more quickly at night (Jin et al., 2018; Tian et a.l, 2019).

2.4 Exploration of Vertical Temperature Profiles

Despite the large volume of literature available on the UHI effect, and the growing body of research on the influence of 3D morphology on air temperature in cities, most research to date has focused on the spatial distribution of heat at the surface level of urban landscapes (Gage & Cooper, 2017; Jin et al, 2018; Lesnikowski, 2014; Tian et al., 2019; Yu et al., 2020). To this point, a majority of the research discussed in this literature review so far has been in the context of land surface temperature. Most monitors at weather stations in and around cities are located at standardized 2m and 10m heights, so it is relatively easy to set up research weather stations for continual data collection at low fixed heights compared to at high elevations. As pointed out in some studies (Barlow, 2014; Dias et al., 2012; Gorlach et al., 2018; Lokoshchenko, 2016), there is only a limited amount of research that has measured or looked at the vertical atmospheric features of the UHI effect, though the number of studies seems to be growing. It may be that the comparative ease of measuring temperatures close to the ground is part of the reason why there is less research on the vertical presentation of UHIs compared to its presentation at or near ground level.

A variety of methods, including satellite imaging, tethered and untethered radiosondes, and sensors affixed to tall structures have been used to investigate vertical temperature profiles. Gorlach et al. (2018), used satellite data to estimate the approximate height of the UHI effect over Moscow. The authors noted, however, that their interpretation of results was limited by the low spatial resolution of the satellite images, and they were therefore unable to look at the fine details of the vertical structure. Despite this, they estimated that the UHI effect could extend as far as 1500m above Moscow in the summer. The authors also noted that their methods were only applicable over a large geographical area, which is not helpful in understanding the microscale structure of local UHI effects. Lokoshchenko et al. (2016) measured vertical temperature profiles over Moscow using a mixture of radiosonde data and sensors affixed to structures including a TV tower and mast, in an attempt to determine the upper boundary of the UHI. The researchers concluded that the UHI extended approximately 400m above the city, at which point temperature anomalies related to the city were no longer statistically significant compared to a rural control location. This is in contrast to the results found by Gorlach et al. (2018), but this difference could be attributed to the low spatial resolution of the latter study's methods. Sugawara et al. (2021) used tethered balloons to investigate the vertical structure of a local cool island above a city park. Their observations appeared to show an increased cool island over the park during the day, but results were considered against surface data from a different year and may have limitations in validity. Radiosonde based methods also come with limitations. Radiosonde data is complicated by the thermal inertia of the sensors, meaning they experience a slight delay in registering the actual temperature and cannot keep up as the radiosonde gains elevation. This leads to a slight

overestimation of temperature (Lokoshchenko et al., 2016). Radiosondes are also difficult to precisely control and present a challenge for obtaining consistent, repeatable data (Adkins, 2020; Lokoshchenko, 2016). And while the use of meteorological masts or other tall structures for affixing sensors to is feasible, researchers must consider the influence of building heat on sensors, and may also face both cost barriers and practical height limitations with regards to how far up they can record data (Adkins, 2020; Masic, 2019).

Another approach to estimating and understanding the vertical structure of the UHI is through statistical modelling. For example, the height of the UHI was estimated using a modelling experiment by Wang et al. (2013), which showed mean temperatures over the Beijing metropolitan area to be comparatively warmer than those over a rural control area. The temperature difference extended up to about 0.8km in the summer, and 0.5km in the winter. This is a similar height to that found by Lokoshchenko et al. (2016), despite the different climatic locations. Barlow (2014) provides an extensive review of progress in modelling of the UBL, including temperature phenomenon like the UHI. While modelling of the urban atmosphere has come a long way, models still lack precision due to an incomplete understanding of the processes within the UBL.

2.5 Studying the Urban Atmosphere with Remotely Piloted Aircraft Systems

Remotely Piloted Aircraft Systems (RPAS, also known as drones or UAVs) are a relatively new tool being used in atmospheric investigations. RPAS have only been applied to vertical temperature investigations in a small number of studies, many of which are feasibility studies. The use of RPAS for the collection of vertical temperature data could eliminate many of the limitations encountered with other methods currently favoured by atmospheric researchers (Adkins et al., 2020; Masic et al., 2019). For obvious practical and safety reasons, small RPAS can bypass the barriers faced by larger, conventional piloted aircraft in studying the lower urban atmosphere. Additionally, the location of RPAS in the sky can be precisely controlled. Controlled RPAS do not encounter the location inconsistencies faced by radiosondes and allow for mounted sensors to remain in position long enough to remove thermal inertia errors. RPAS are also able to hover far enough away from structures to eliminate building interference in temperature recordings. Of particular importance is the relative low cost and ease of accessibility of small RPAS, enabling their broader use within the research community. In a feasibility study by Masic et al. (2019) a small, in-house designed multirotor RPAS apparatus was used to investigate vertical temperature profiles over Sarajevo, in the pursuit of a cost effective, flexible methodology for measuring atmospheric inversions over an urban area. This feasibility study was able to capture temperature changes over a vertical distance of 1km, and

effectively identified temperature inversions[4]. In addition, the study presented a correlation of low-level inversions (150m or below) with high concentration particulate matter pollution events, demonstrating that inversions trap air pollutants within the RSL. Adkins et al (2020) presented a methodology for using "meteorologically instrumented unmanned aircraft systems" to investigate the UBL, including parameters such as temperature, pressure, and wind speed. However, the authors also noted a current limitation of RPAS: that the existence of tight regulations regarding flights within urban areas can restrict the possible breadth of available measurements, especially height restrictions.

Other studies have investigated air temperature and other meteorological parameters in the ABL using RPAS, though not in relation to the UBL. Kroonberg et al. (2012) explored the feasibility of using an RPAS to measure the spatially averaged temperature structure of the ABL over a heterogenous surface, and compared it to other more well-established atmospheric measurement techniques such as sondes. The authors found the RPAS to be a reliable and promising new technology. Martin et al. (2014) successfully used a mini-RPAS to observe entrainment processes in the transition area between the ABL and the overlying stably structured free atmosphere at high resolution. Dias et al. (2012) tested the applicability of a mini-RPAS for measuring ABL features that are difficult to obtain in other ways due to their elevation, such as ABL height, and entrainment sensible virtual heat flux. The authors found that humidity and temperature profiles were also easily obtained at high resolution using the RPAS system.

2.6 Literature Review Summary

Available literature on the urban heat island and the urban atmosphere in general continues to expand. While some causes of the UHI such as the thermal properties of materials, impermeable surfaces, and vegetation are well understood, other factors are newly emerging. Research into the role of the 3D urban environment on land surface temperatures has uncovered several important and probable cause-effect relationships between neighbourhood design and the UHI. Furthermore, the interplay of heat promoting surface properties and urban air flow in the atmospheric regions above urban neighbourhoods is important in pollution and heat management. However, there is still a clear lack of data characterizing the vertical air temperature profile of urban microclimates. This gap underlines the need for additional research into vertical temperature profiles within cities; especially as they relate to neighborhood scale features, the UBL, and their effect on the formation of UHIs. It is clear that RPAS are emerging as a promising new tool for measuring the meteorological parameters of cities. These small airborne vehicles are poised to play a key role in improving our

[4] A temperature inversion is a reversal in the direction of atmospheric temperature change with increasing altitude. Normally, temperature decreases with altitude, but will increase with altitude in an inversion layer.

understanding of the UHI, its role in human health, and how we can better manage urban design principles to combat it. Consequently, the following study aims to investigate vertical temperature profiles within a dense, downtown metropolitan area using RPAS, with the goal of observing how atmospheric temperature might vary on a microclimatic scale in relation to each site's 2D and 3D surroundings.

3.0 Methods

This project utilized an experimental research design. The methodology included direct atmospheric profile measurements, results analyses and the graphical and numerical presentation of atmospheric temperature profiles.

Four locations were chosen within and around downtown Vancouver in order to capture a variety of different surfaces, materials, and urban morphologies. All locations fall within a fairly small geographic area of approximately 10km^2, which allows for an analysis of variability in atmospheric vertical temperature profiles due to urban morphology, vegetation, and surface material type rather than horizontal distance between locations. Locations were chosen to represent the following four types of urban environment.

1. **Mediumly urbanized**. Mix of low and higher rise buildings and streets, with moderate vegetation, grass/park and tree cover, and a higher proportion of lighter colored pavement or gravel. Residential or mixed residential/commercial.
2. **Highly urbanized**. Includes many tall and medium sized buildings and streets, lots of asphalt, concrete, and other man-made surfaces, with little vegetation or tree cover.
3. **Urban with UHI mitigation features**. An urbanized location with buildings, streets, and man-made features, but also features such as green roofs or walls, higher integration of parks/grass/gardens, and low albedo materials.
4. **Urban parkland**. A highly vegetated area with a large proportion of trees/grass/shrub or other natural features, and minimal man-made features.

The sites chosen to represent each of the above four categories are shown on Google Earth satellite images included below in Figures 2 through 5. Exact locations of each site are as follows:

1. Intersection of Denman Street and Morton Avenue, near the public art sculptures
2. Intersection of Seymour Street and Nelson Street, in the Impark parking lot #83.
3. Jack Poole Plaza, near the Cactus Club and Convention Centre West green roofs
4. Middle of SW Vanier Park, near Chestnut Street and Creelman Avenue

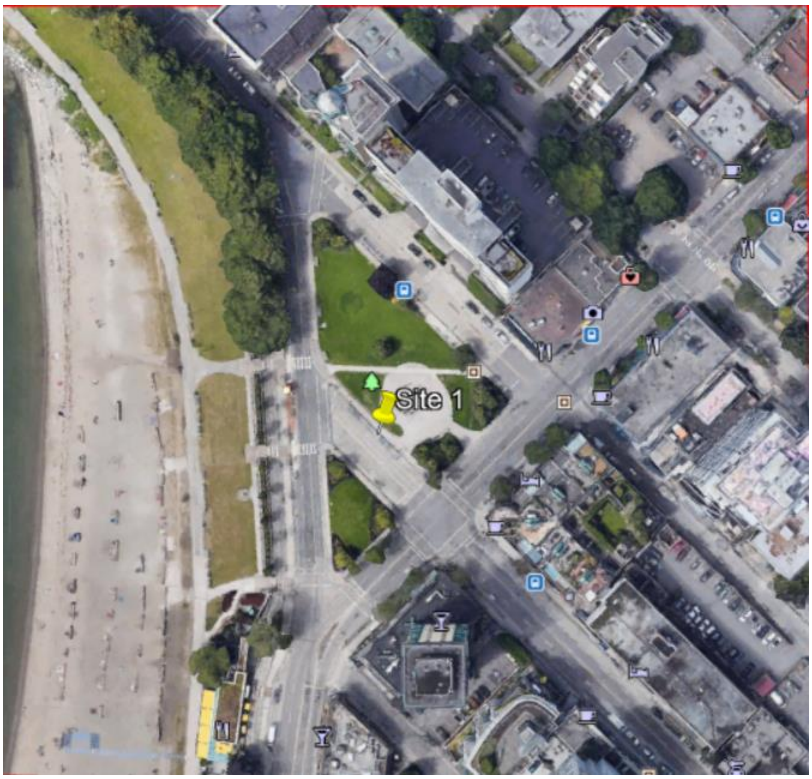

Figure 2: Google Earth Image of Site 1 - Denman St. and Morton Ave

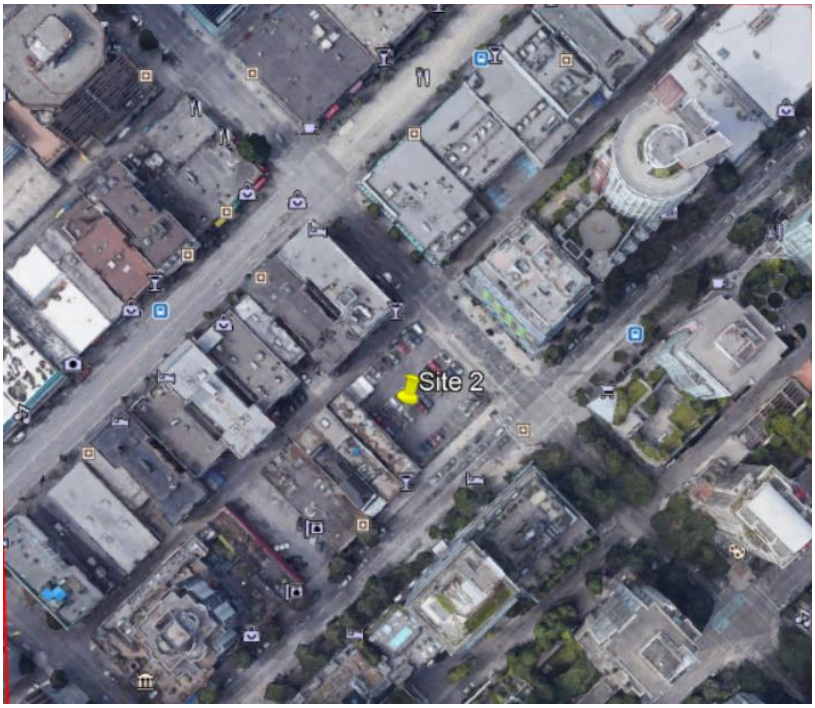

Figure 3: Google Earth Image of Site 2 - Seymour St. and Nelson St. in parking lot #83

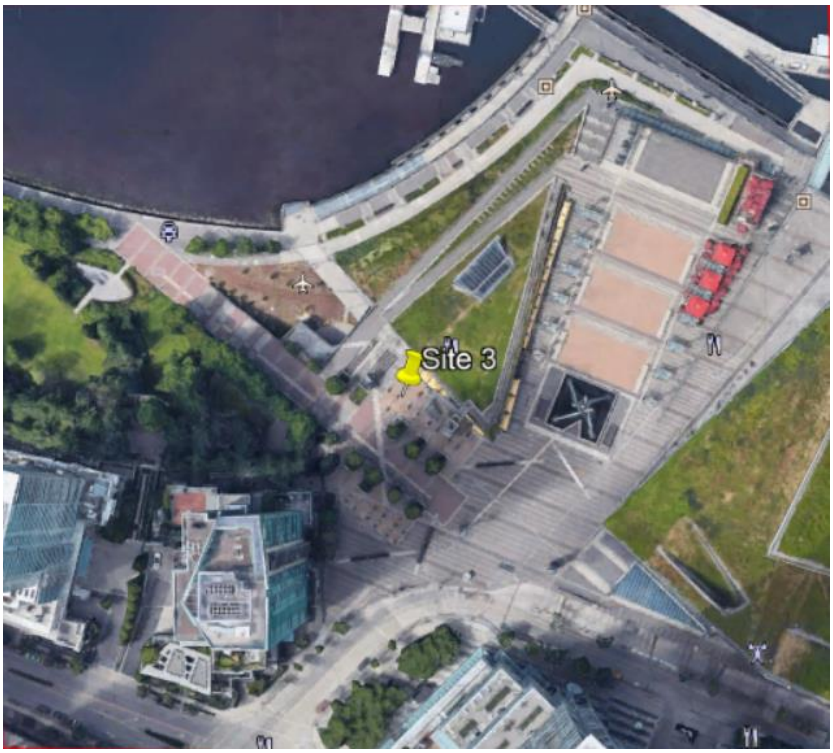

Figure 4: Google Earth Image of Site 3 - Jack Poole Plaza near the Convention Centre West

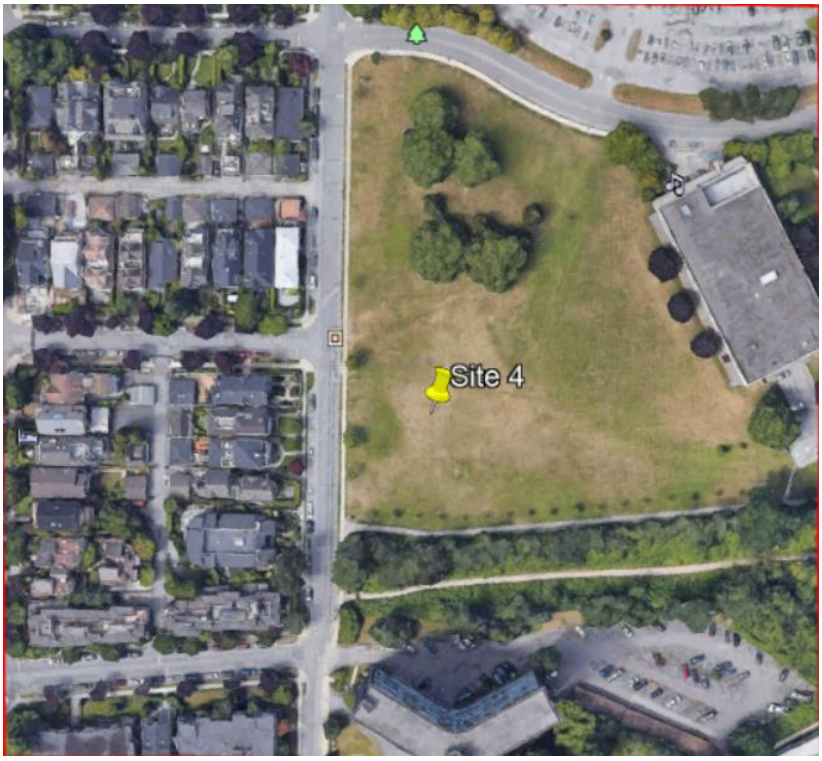

Figure 5: Google Earth Image of Site 4 - SW Vanier Park at Chestnut St. and Creelman Ave

It should be noted that because all of downtown Vancouver is within Class C controlled airspace, some limitations were encountered in choosing the locations for testing due to regulations concerning the use of RPAS within such airspace. All flights must be conducted within Transport Canada regulations, and certified pilots are required to request individual approval for their flights from NAV CANADA and the Harbour Control Tower. In addition to flight permissions, RPAS should be flown approximately 9m (30ft) away from residential windows due to privacy concerns. This was something that had to be considered at any sites near mid- or high-rise apartment buildings. Finally, flights carried out in municipal and provincial parks, as well as on private property, require written permission from the property or landowners/managers prior to commencement. Given these constraints, the sites for this study were selected to be on public property whenever possible, and a reasonable distance away from residential homes and buildings.

At each testing site two RPAS were employed in order to capture temperature data at four different altitudes, as well as at ground level. Each RPAS rested at ground level (1m from ground surface) at the start of data capture for a minimum of 10 minutes, launched and then hovered at two separate altitudes for 6-10 minutes per altitude. Data was collected at the following elevations above ground: 1m (ground height), 20m, 40m, 70m, and 120m. In Canada, 122m is the maximum allowable altitude for drone flights without a special flight operations certificate (SFOC), which was not obtained for this study. In some cases, pilots received individual height restrictions of 90m, so in those cases the maximum height obtained was limited by NAV CANADA permissions; however, this was out of our control. The range of altitudes chosen was intended to capture the top of the urban canopy layer even in the middle of downtown, where the highest average building height is located.

The decision to have each drone travel to and hover at a set altitude rather than ascend the entire distance at a set velocity was made in order to allow sufficient time for the attached temperature sensors to adjust and overcome any thermal inertia. The temperature sensors used were the TMCx-HD Air/Water/Soil Temperature Probes, which have a response time in air of two minutes. The RPAS used in this study were the DJI Air, Mavic 2 and Phantom 4 Pro. All are small, multi-rotor (4) drones with a typical maximum flying time of 20 minutes based on battery life. The battery life was used to inform the selection of a 6 to 10-minute hover time, which allowed ample time for the sensor to adjust and provided a safety margin in case total flying time was significantly shorter than the maximum due to individual age of the RPAS battery or adverse wind and weather conditions. Each sensor was connected to a HOBO U12-013 data logger, and housed in a small, lightweight metal dish. The housing apparatus was approximately 8cm deep, with the data logger and sensor resting on a 2cm thick layer of foam to provide insulation from any heat produced by the body of the RPAS. The sides of the metal housing also provided protection from air currents created by the RPAS rotor blades and from

direct solar insolation. Each sensor apparatus was then secured to the underside of the RPAS and launched from a small platform. The platforms were made with a space cut out from the centre to allow the sensor apparatus to rest freely beneath the RPAS and collect pre-launch data without contacting the ground surface.

Data was collected twice on each sampling day: once in the mid-morning at 10am, and once in the mid-afternoon at 3pm. These times were intended to capture any temporal variation of atmospheric temperature over the course of the day. In the morning, air temperatures should be cooler as the sun has only been out for a few hours. However, as the day continues and the sun heats the surface of the city, subsequent variation in air temperature is expected due to heat absorbed and reradiated by surfaces and materials. Therefore, the data collection at 3pm was intended to approximate the hottest part of the day in order to capture maximum temperature variation.

Testing was completed over a period of 8 months. Originally, data was intended to be collected in three seasons: late summer, winter, and spring. The purpose of collecting data over a longer time period was to capture seasonal and diurnal variation in the atmospheric temperature profiles. Temperature variation between sites related to the characteristics of each was expected to be more pronounced during the summer months when temperatures are higher overall. However, the literature implies that the UHI effect still exists in the winter months, though to a lesser degree (EPA, 2008; Gorlach, 2018; Lokoshchenko, 2016). Data collection over multiple seasons thus allowed for observation of seasonal variability and an analysis of whether the UHI effect was present and persistent across seasons. It also allowed for the collection of important additional data points for analysis at each location. Unfortunately, prior to the last round of data collection in the spring, a safety issue related to the ability of the drones to carry the sensor apparatus payload was encountered. This issue compromised the ability of the research team to safely complete the last round of flights, which therefore had to be cancelled. As a result, data was only collected for two seasons: fall/late summer, and winter

Data collection dates were targeted to capture temperatures representative of typical seasonal weather in Vancouver: late summer/early fall (warm, sunny weather), winter (cold, overcast weather), and spring (mild, cool to warm weather). Mid-summer data representing hot and humid weather was not collected due to the constraints of the academic year, which runs from September to April. As such, the late summer measurements were selected to target warmer days resembling summer temperatures as much as possible.

Typical weather in Vancouver for this pilot study was defined as an approximation of average ground level atmospheric temperatures for the first and second month of each season, as outlined in Table 1 below. The exception to this was the summer/fall season, for which an

approximate average was determined spanning both seasons, specifically the end of summer and beginning of the fall. In order to approximate summer as much as possible, a warmer day was targeted within that range, as noted above. Also as noted above, the spring testing date was cancelled.

Table 1: Average Seasonal Temperatures for Vancouver Based on the First Two Months of Each Season (Source: Environment Canada, 2020)

Season	Duration	Targeted Sampling Time	Ave Temp (^{o}C)
Summer/Fall	Sep. 1 – Nov. 30	Late September to early October	15-20
Winter	Dec. 1 – Feb. 28	Mid January	5-10
Spring	March 1 – May 31	Late March to early April (cancelled)	9-14

In addition to the collection of temperature data at each location and over two seasons, observational and weather data was also collected. Photographic documentation of each site at the time of testing was captured, as well as written observations related to the types of surfaces beneath and around the launch sites, as well as the quantity, type and condition of vegetation in the immediate area, and the general weather conditions at the time of launching. Other data of note, such as issues with flights or on the spot changes in response to unexpected events were also recorded. Weather data was retroactively collected from the nearest Environment Canada weather station (Vancouver Harbour CCS) for both of the two launch times on each day, including: temperature, relative humidity, wind speed and wind direction (Environment Canada, 2021). Weather station data can be found in Appendix A, and was used to double check validity of data and to confirm weather conditions on the testing days. Given that some variability was expected between sites and the nearest weather station, a margin of error of up to ±4°C was considered acceptable.

To characterize the materials, surfaces, and urban morphology of each site, the proportion and type of materials and vegetation present at each location was quantified. The site area was defined as a 0.25km x 0.25km square centered over the launch location. Satellite images from Google Earth, in combination with data from the City of Vancouver's Urban Forest Strategy (2018), were used to approximate the percent tree canopy coverage within each area, as well as the percent coverage by impervious surfaces. Additionally, Google Earth satellite images were used to approximate the amount and type of different kinds of surface materials within each site area. Types of surfaces considered include roof color (dark, light, or green roofs), asphalt, concrete, gravel, paving stones, grass/low vegetation, and trees. Following surface type identification, corresponding albedo and emissivity values for each material type was also noted. Finally, in addition to types of surfaces, the intensity of urban morphology was

categorized for each site. Urban morphology categorization is based on average building height at the site (this is also the measure of UCL height), observed density of buildings, and the number of low (under 7 floors), medium (7-15 floors), and tall (over 15 floors) buildings present within the site area. Buildings that were more than 50% within the site bounds were included in the building count. Any other major urban morphology features of note were also considered, such as the location of buildings relative to wind or ocean exposure.

Collected data was compiled and displayed visually using graphs and tables for comparison and analysis. Air temperature at each altitude was determined by taking the average of temperatures logged by the sensor after the first 2.5 minutes at each altitude, during which time the sensor would be adjusting. To ensure data was only taken from the intended altitude and not during ascent or descent, the first and last 30 seconds of hovering at each altitude was excluded from data consideration. Examples of unaveraged data from several altitudes prior to averaging is provided in Appendix B. Average air temperature was then plotted against altitude at each site and for each launch to obtain a graphical representation of the environmental lapse rates[5]. The lapse rate at each site and for each date and launch time were also compared against the dry and moist adiabatic lapse rates[6] (DALR and MALR, respectively) to determine atmospheric stability. Vertical temperature profiles were compared between sites and analyzed based on the characteristics of each site using a simple observational analysis. The goal was to characterize the vertical temperature profile of each location, understand if and how it varied between sites, and then explore possible correlations between the characteristics of each site and the temperatures profiles found there.

In parallel to the collection and analysis of data from each site, a review of Ecocity Builders 18 standards was undertaken to inform a discussion of results within the context of holistic, eco-city planning. Additionally, a review of the City of Vancouver's Greenest City Action Plan and Urban Forest Strategy, as well as Metro Vancouver's Climate 2050 regional framework were conducted. Major findings from the study are discussed in the context of these regional and local frameworks with the goal of understanding how Vancouver and the lower mainland regional area may benefit from the information and how it can be applied to improving the city's resilience to climate change.

4.0 Results

This section provides a description of the observations and data collected during the two testing sessions. To start, the physical characteristics of each of the four sites are discussed.

[5] Lapse rate is defined as the rate of temperature change with increasing elevation

[6] The dry adiabatic lapse rate (DALR) is the rate at which dry air cools with altitude, specifically 10°C/km. The moist adiabatic lapse rate (MALR) is the rate at which saturated air cools with altitude, and is roughly 6.5°C/km

This includes both an overview of surface types, and quantitative rankings of each site based on the quantities of different types of surfaces and features. Specific attention was paid to vegetation, impervious surfaces, buildings, and material properties. Following the site descriptions, data from the summer testing day is presented, followed by data from the winter testing day. Within each season's subsection, observed trends are noted, and visual representation of the data is provided in both graphical and tabular formats.

4.1 Site Characterization

Each of the four sites was characterized by quantifying the proportions of different types of materials and vegetation coverage within the predetermined site area. Additionally, the distribution of surrounding building heights was also used to characterize the area. Finally, the location of each site relative to prevailing wind and proximity to the ocean was considered. A summary of site characteristics is included in Table 2.

Site 4, which was located in Vanier Park and chosen to represent the greenest and least urbanized area, had the highest percentage tree canopy (20%) and vegetation coverage (49%) of all the sites. Site 4 also had the lowest overall building height, with no tall buildings and only 1 medium height building. Site 4 was adjacent to a residential neighbourhood with RT zoning to the west, made up of primarily one and two-family dwellings, which account for approximately 40% of the site area. To the farthest south end was the only medium height building, located in a RM zoning district for low to medium density mixed residential. The remainder of the site is occupied by grass and trees that make up an urban park. The average building height of Site 4, and thus the height of the UCL, was calculated to be 10.1m, though this may be skewed slightly due to the existence of the single 14 story building at the south end of the site, when all other buildings are a maximum of 3 stories tall. Therefore, the UCL can be considered to be 8.9m in the northern upper two thirds of the site area. Site 4 is located about 0.5km from the Burrard Inlet to the north.

Despite having the most vegetation coverage, Site 4 did not have the lowest proportion of impervious surfaces, or the lowest proportion of dark roofs and asphalt. Dark roofs and asphalt have the lowest albedos of those identified, and some of the highest emissivity values. In fact, Site 4 had the second highest proportion of dark roofs (25%), and the second lowest proportion of asphalt (21%) of all the sites.

Site 2 was located in a parking lot at the intersection of Nelson Street and Seymour Street, in the heart of the commercial district of downtown. This site was selected to represent the most urban and man-made landscape, with the highest predicted risk for UHI effects of the four sites. Site 2 had the most impervious surface coverage (83%) and the lowest vegetation coverage (16%). Most of the vegetation coverage at this site was provided by trees, which are concentrated to the SE corner of the site where all of the tall buildings – primarily high-density residential apartment complexes – are located. Site 2 had the highest number of total buildings (38), and the highest number of tall and medium height buildings. Despite this, the average

building height of Site 2 was only calculated to be 22.3m, likely due to also having a large quantity of low buildings between 2 and 3 stories. Of the 38 buildings included in the site area, 30 of them were classified as low buildings. The NW two-thirds of Site 2 was comprised mostly of these low, commercial type buildings with flat, dark roofs and barely any trees or vegetated surfaces. The flight location itself was centered over the parking lot in the middle of the site, with the apartment complexes to the SW and the low commercial buildings bounding the rest of the site to the north and east.

Table 2: Summary of Site Characteristics at all Four Testing Locations

	Site 1 - English Bay		**Site 2 - Parking Lot**		**Site 3 - Convention Centre**		**Site 4 - Vanier Park**			
General Features	Site data	Vancouver data	Site data	Vancouver data	Site data	Vancouver data	Site data	Vancouver data		
% Tree Canopy Coverage	9	10-20	12	<5	11	5-15	20	15-20		
% Vegetation Coverage (all types)	21	-	16		29		49			
% Impervious Surface Coverage	59	50-75	83	>75	27	25-50	50	25-50		
Urban Morphology Features										
Observed Density	Medium		High		Medium- low		Low			
Average Building Height (m)	24.5		22.3		81.7		10.1			
Tall Buildings (>15 floors)	4	21%	6	16%	3	60%	0	0%		
Medium Buildings (7-15 floors)	1	5%	2	5%	0	0%	1	3%		
Low Building (<7 floors)	14	74%	30	79%	2	40%	33	97%		
Total # Buildings	19		38		5		34			
Surface Material Types:	%								Albedo	Emissivity
Dark roof	15%		37%		3%		25%		0.1	0.92
Light roof	8%		14%		4%		1%		0.4	0.9
Green roof	2%		3%		14%		0%		0.2	0.93
Asphalt	30%		27%		10%		21%		0.08	0.95
Concrete	6%		5%		10%		3%		0.225	0.8
Gravel/Paving Stones	2%		0%		23%		2%		0.15	0.9
Grass/Low Vegetation	10%		1%		4%		29%		0.25	0.93
Trees	9%		12%		11%		20%		0.165	0.97
Other	19%		1%		22%		1%		N/A	N/A

Interestingly, the tree canopy coverage at Site 2 (12%) was not the lowest of the four sites, having a slightly greater proportion of tree canopy coverage than both Sites 1 (9%) and 3 (11%) by several percent. It should be noted that because percent coverage of materials was estimated with a grid method using Google Earth images, there is a chance the percentage difference is due to estimating error. For this reason, Sites 1, 2 and 3 could be considered to have approximately the same amount of tree canopy coverage. Despite the similar tree coverage, Site 2 still boasts the lowest total proportion of vegetation.

Sites 1 and 3 fall somewhere in the middle between the above two mentioned sites, with varying vegetation and material coverage. Site 1 was located in a small green area 120m to the east of English Bay Beach, near the intersection of Morton Ave and Denman Street. Site 1 is the most exposed to prevailing ocean breezes, which originate from the west and northwest in the summer. This site is located in the West End, a residential mixed zoning neighbourhood generally known for its amenities and lush greenery. Despite this, Site 1 has the lowest tree canopy coverage (9%). This is partially due to the large amount of beach included in the site area, and the site's proximity to several blocks of commercial zoning to the SW, which have lower than average tree canopy coverage relative to the rest of West End (City of Vancouver, 2018). Site 1 has the second lowest overall vegetation coverage (21%) after Site 2, and the second highest impervious surface coverage (59%). The building distribution of Site 1 is fairly mixed, having 19 total buildings within its area, 4 tall, 1 medium height, and 14 low height. The average building height at Site 1 was calculated to be approximately 24.5m.

Site 3 is the last site to be discussed and was chosen because of the presence of two large green roofs within its bounds in an effort to observe the mitigation potential of such features. Site 3 is the northern most site, located just to the west of the Vancouver Convention Centre West Building. This site is the closest to the ocean, being only 70m away, but is somewhat sheltered from prevailing winds that blow from the west and northwest and which would have to pass through the dense downtown area first. This site also has the lowest overall number of buildings, 5 in total. Despite the small number of buildings, observed site density was still rated as medium-low because three of the buildings were either dense high-rise apartment complexes or commercial skyscrapers. Due to the existence of the tall buildings, average building height for the entire site was calculated to be approximately 82m. However, given the distribution of buildings across the site this may not be accurate. Instead, the average building height in the SW corner should be considered to be 129m, and for the rest of the site, 10m.

Site 3 has relatively good vegetation coverage, with the second highest percent coverage of the four sites (29%). Most of the vegetation coverage at this site is from lower vegetation such as grass covering the green roofs, while the tree canopy coverage at Site 3 is the second lowest overall (11%). Site 3 also boasts the lowest proportion of impervious surfaces (27%). It should be noted, though, that 23% of the site is covered by paving stones, which have a lower degree of permeability compared to gravel and grass/surface vegetation.

4.2 Summer Vertical Profiles

Vertical temperature profiles varied significantly between all four sites in the summer time, both during the morning and afternoon launch times. Variation between the individual lapse rates at each site demonstrated the different atmospheric structures above each site. Variation also existed in the temperatures between sites. The maximum difference in air temperature occurred in the afternoon at 40m, between Sites 1 and 2, with a difference of 3.36°C. Surface temperatures also varied between sites, with the largest difference of 3.06°C occurring between Sites 1 and 4. When considering both air and surface temperatures together, the greatest variation occurred between the 40m air temperature at Site 3 and the surface temperature at Site 4, in the morning. This difference totaled 4.03°C.

In the morning time, overall variation in air temperatures between sites was lower, and temperatures appeared to converge at the highest altitude of 120m. This is in contrast to the afternoon, where variation between sites was slightly greater overall, and temperatures did not converge at the 120m mark, though they did appear to start moving closer together. Vertical profiles from all sites are shown in Figure 6 and Figure 7.

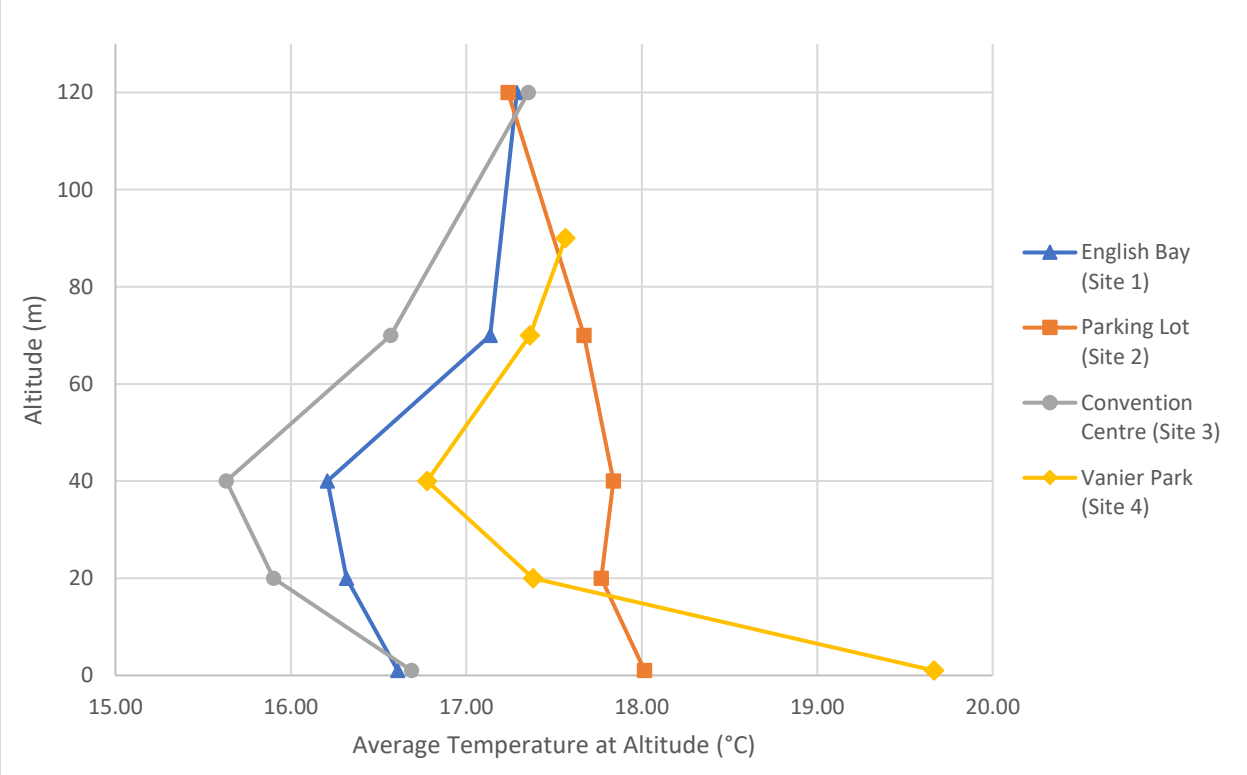

Figure 6: Combined vertical profiles of the atmosphere at all sites, morning launch (10am), summer

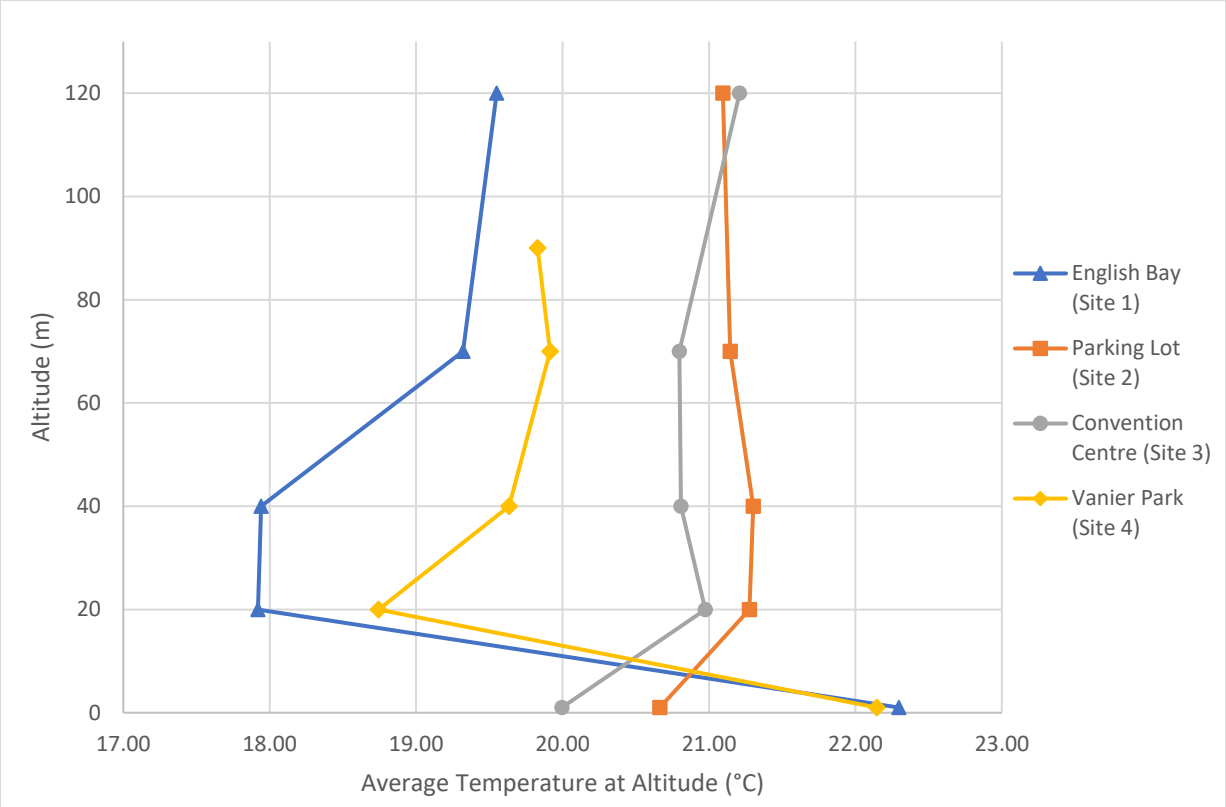

Figure 7: Combined vertical profiles of the atmosphere at all sites, afternoon launch (3pm), summer

Site 2 – the parking lot – displayed the warmest air temperature overall in both the morning and afternoon, though the surface temperature at Site 2 was only the second highest in the morning, and the third highest in the afternoon. Interestingly, the park location at Site 4 had the highest surface temperatures during both launches. At altitude, however, air temperatures at Site 4 were generally lower, and remained lower even through the increasing heat of the afternoon.

Both Site 2 and Site 4 displayed minimal change in atmospheric structure from the morning to the afternoon, with the biggest change for each being an increase in temperature, as shown by a shift of the vertical profile to the right. At Site 4, the sharp decrease in temperature seen from the surface to the lower altitudes might suggest that the atmosphere above the site was quite unstable just above the ground. An unstable atmosphere is indicated by a lapse rate that is steeper (or greater) than the DALR, whereas a stable atmosphere has a lapse rate that is less than the MALR; anything between these two rates is considered conditionally unstable. Both the morning and afternoon profiles of Site 4 also appear to show a low-level inversion, starting at 40m in the morning and sinking to 20m in the afternoon. This inversion decreased in thickness over the morning to afternoon time period. Conversely, the parking lot location (Site 2) was the only site which retained a stable atmosphere throughout

the day and did not exhibit any kind of obvious atmospheric inversion, instead having a possible, very minor ground-based inversion in the afternoon. A ground-based inversion occurs when cooling from the surface is trapped beneath a warmer layer of air above it. Figure 8 shows an example of the vertical profiles of Site 2 and 4, respectively, in the afternoon. Both profiles have been plotted against both the DALR and the MALR to determine stability. A compilation of all independent vertical profile graphs alongside the DALR and MALR is included in Appendix C.

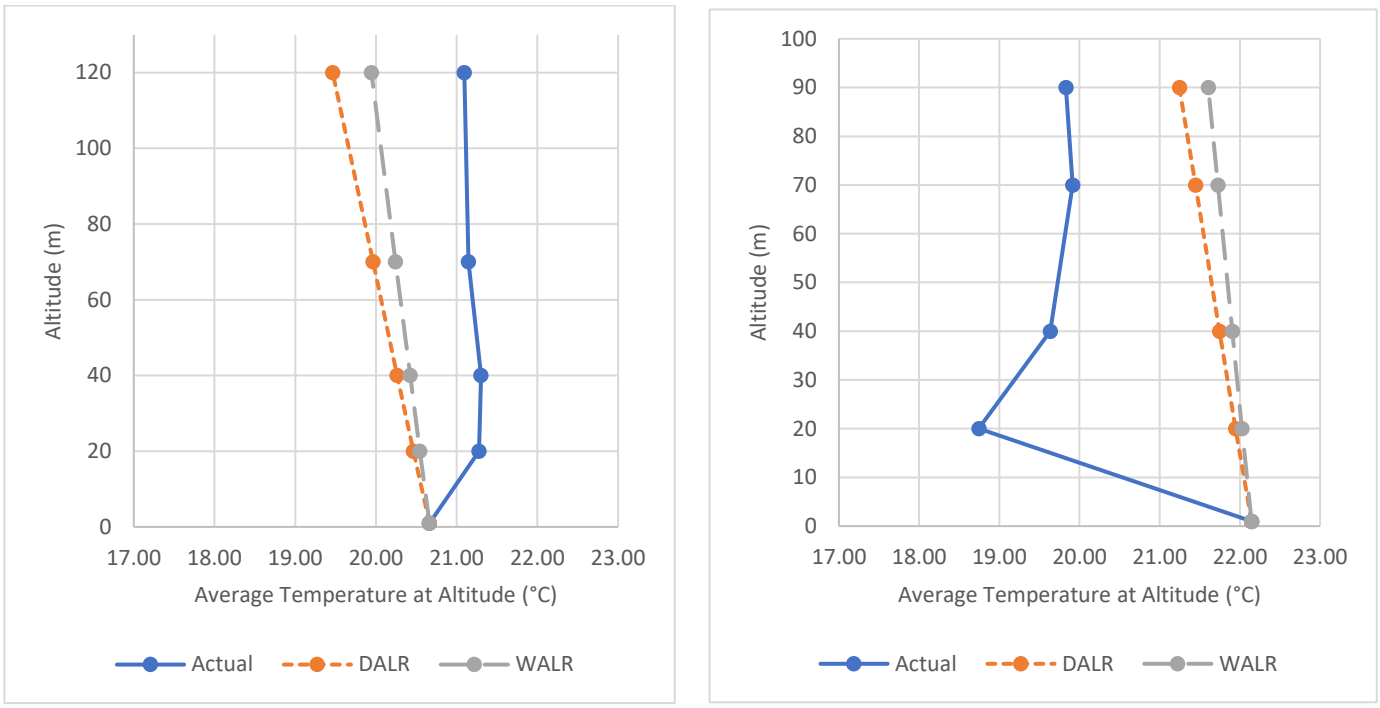

Figure 8: Vertical profiles of atmosphere at Site 2 (left), and Site 4 (right) during the afternoon launch at 3pm, summer, with accompanying DALR and MALR

In contrast to Site 2 and 4, the Convention Centre site (Site 3), showed considerable change throughout the day. In the morning, Site 3 was the coolest of the four sites through almost its entire vertical height, and was very close to being the coolest at the surface; the difference between Site 3 and the coolest site (Site 1) was less than 0.1°C. The morning atmospheric profile at Site 3 was unstable low in the atmosphere, and displayed a considerable inversion layer from 40m and above. Site 3 also had the lowest overall air temperature measured that day at 15.63°C. However, in the afternoon the atmospheric temperature profile of Site 3 changed considerably. At the surface level, Site 3 was the coolest at 20.0°C, but once in the air was established as the second warmest site overall. This site also displayed a ground level inversion to 20m, followed by a fairly steady temperature through 40m and 70m, with a slight uptick in temperature to 120m. This slight increase in the upper part of the measured

atmosphere may indicate the beginning of a higher altitude inversion that was beyond the reach of the data collected for this study.

Site 1, at English Bay, was also peculiar compared to the other sites. In the morning, the English Bay site was one of the cooler sites, with a very similar atmospheric structure to Site 3, albeit slightly warmer by about 0.6°C. In the afternoon, the surface temperature of Site 1 warmed substantially to become the warmest surface location overall, whereas the air above Site 1 was in fact the coolest of the four sites. The temperature of Site 1 decreased from 22.30°C at ground level to 17.92°C at an altitude of 20m, a drop of over 4.38°C through a very unstable region. From the 20m point, air temperature was steady for a short time, and then entered an inversion from 40m and beyond.

Surface and atmospheric temperatures with corresponding altitudes for the summer launches, which were completed on September 30, 2020, are provided in numerical form in Table 3 below.

Table 3: Numeric Temperature Profile Data vs. Altitude at all Sites, Summer Launches, Sep. 30, 2020

	Site 1 – English Bay		**Site 2 – Parking Lot**		**Site 3 – Convention Centre**		**Site 4 – Vanier Park**	
Morning, 10am	Average Temp (°C)	Altitude (m)	Average Temp (°C)	Altitude (m)	Average Temp (°C)	Altitude (m)	Average Temp (°C)	Altitude (m)
	16.6096	1	18.0162	1	16.6880	1	19.6657	1
	16.3179	20	17.7698	20	15.9016	20	17.3810	20
	16.2088	40	17.8379	40	15.6321	40	16.7762	40
	17.1371	70	17.6716	70	16.5689	70	17.3627	70
	17.2882	120	17.2377	120	17.3539	120	17.5657	90
Afternoon, 3pm	Average Temp (°C)	Altitude (m)	Average Temp (°C)	Altitude (m)	Average Temp (°C)	Altitude (m)	Average Temp (°C)	Altitude (m)
	20.6641	1	20.6641	1	19.9952	1	22.1456	1
	21.2756	20	21.2756	20	20.9737	20	18.7433	20
	21.3021	40	21.3021	40	20.8077	40	19.6358	40
	21.1457	70	21.1457	70	20.7978	70	19.9151	70
	21.0957	120	21.0957	120	21.2090	120	19.8303	90

4.3 Winter Vertical Profiles

Overall, variation in the vertical temperature profiles between sites during the winter time was much less substantial compared to summer variations. Small temperature differences between the site profiles were present, but the atmospheric structure above all of the sites was

quite similar. As a general trend, in the morning all profiles are warmest at the ground surface, ranging from 5.55°C at the Convention Centre (Site 3) to 6.31°C at English Bay (Site 1). As height increased, temperatures decreased most steeply in the first 20m of the atmosphere, indicating an unstable lower region. At 40m, all profiles experienced a slight decrease in their lapse rates, but still continued to decrease in temperature with elevation, through to the maximum recorded height of 120m. At 120m, Site 4 overtook Site 3 for the lowest air temperature (4.06°C), and Site 1 continued to have the highest air temperature (4.89°C). Throughout the entire vertical profile, temperature differences between the Sites 1, 2, and 4 remained fairly steady.

In the afternoon, the profiles were fairly similar to the morning, with a bit more variation between sites relative to the morning profiles in the 20-70m layer. Beyond the 70m mark, all temperature profiles again continued to decrease until the 120m altitude. Surface temperatures in the afternoon were slightly closer together, ranging from 7.96°C at Vanier Park to 8.39°C at English Bay. At 120m, temperature varied from 6.17°C at Site 4 to 6.7°C at Site 2. A graphical representation of the vertical profiles at all sites are included in Figures 9 and 10.

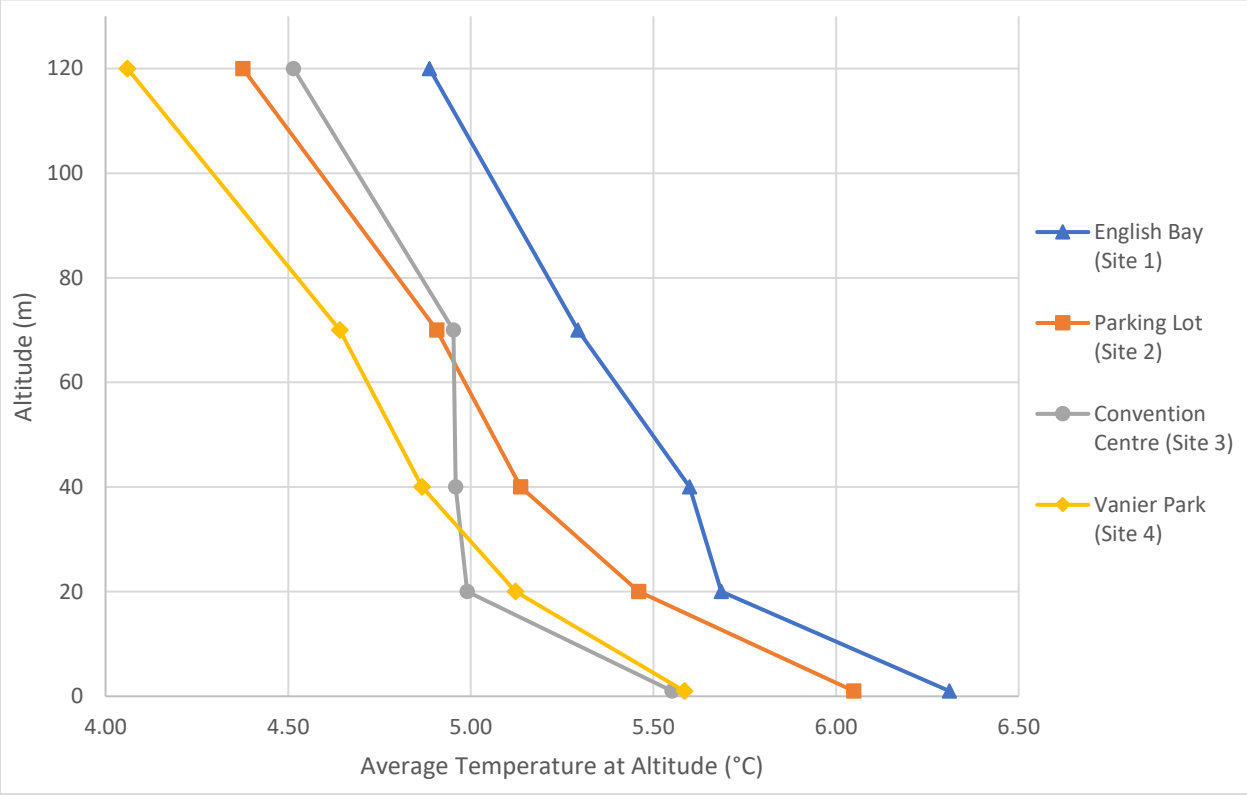

Figure 9: Combined vertical profiles of atmosphere at all sites during the morning launch (10am), winter

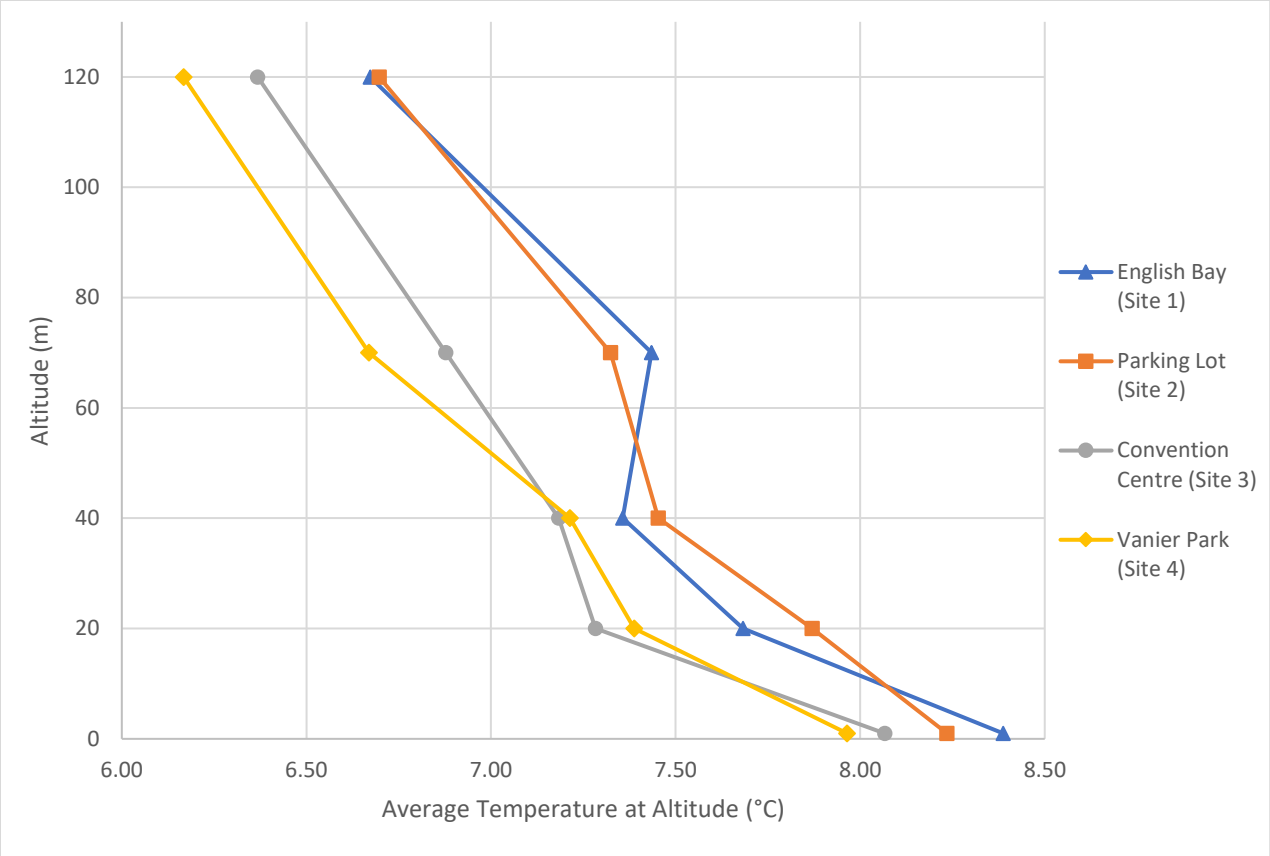

Figure 10: Combined vertical profiles of atmosphere at all sites during the afternoon launch (3pm), winter

During both the morning and afternoon launches, Sites 3 and 4 both competed for the lowest overall temperature. The exception to this was above 40m in the morning, where the Convention Centre (Site 3) experienced a period of steady temperature which resulted in the air temperature being warmer than that of Site 4 in the upper levels of the urban atmosphere. Beyond 70m in altitude, the atmosphere above Site 3 again began to cool with height at a similar rate to the other sites.

Site 1 at English Bay was the warmest of the four sites, at least in the morning time. In the afternoon, Site 1 and 2 competed for warmest temperature profile, with atmospheric profiles overlapping each other at various altitudes. Site 1 also displayed the only potential inversion observed during the winter launch, though it was very slight. Due to the small difference in temperature (0.08°C) between 40m and 70m over Site 1, it is uncertain whether this was truly an inversion or merely a localized perturbation in temperature.

Stability of the atmosphere seemed fairly consistent across sites. In both the morning and afternoon, an unstable layer existed closest to the ground, ranging up to about 20-40m. In the middle reaches of the measured urban atmosphere (20-70m), stability increased briefly,

with all sites experiencing a layer of stability somewhere in this region. In the upper section of the measured column, all profiles again became unstable or conditionally unstable.

Surface and atmospheric temperatures with corresponding altitudes for the winter launches, which were completed on January 29, 2021, are provided in numerical form in Table 4 below.

Table 4: Numeric Temperature Profile Data vs. Altitude at all Sites, Winter Launches, January 29, 2021

	Site 1 – English Bay		**Site 2 – Parking Lot**		**Site 3 – Convention Centre**		**Site 4 – Vanier Park**	
Morning, 10am	Average Temp (°C)	Altitude (m)	Average Temp (°C)	Altitude (m)	Average Temp (°C)	Altitude (m)	Average Temp (°C)	Altitude (m)
	6.3105	1	6.0486	1	5.5512	1	5.5846	1
	5.6856	20	5.4596	20	4.9903	20	5.1222	20
	5.5993	40	5.1363	40	4.9581	40	4.8666	40
	5.2933	70	4.9068	70	4.9522	70	4.6418	70
	4.8868	120	4.3760	120	4.5147	120	4.0600	120
Afternoon, 3pm	Average Temp (°C)	Altitude (m)	Average Temp (°C)	Altitude (m)	Average Temp (°C)	Altitude (m)	Average Temp (°C)	Altitude (m)
	8.3872	1	8.2352	1	8.0663	1	7.9644	1
	7.6824	20	7.8700	20	7.2830	20	7.3877	20
	7.3572	40	7.4531	40	7.1837	40	7.2142	40
	7.4352	70	7.3243	70	6.8779	70	6.6698	70
	6.6726	120	6.6968	120	6.3680	120	6.1673	120

5.0 Discussion

An analysis and interpretation of the data collected during this study is presented in the following section. Results are first discussed from the summer testing day, then from the winter testing day. For both days, data from the morning is analysed before data from the afternoon, and then a review of general observations from the entire day is provided. Potential sources of error are also considered. Finally, the results of the study are discussed in the context of Ecocity Strategies, and compared against the current strategies and frameworks of the region. This includes strategies from the City of Vancouver and from the larger Metro Vancouver Region.

5.1 Summer Vertical Profiles

An examination of the data from the summer testing day revealed some results that aligned with the hypothesis of the researchers, and some results that were unexpected. In this

section, the observed influence of site features on vertical profiles will first be discussed for the morning flight, followed by the afternoon flight observations, and finally a review of general observations for the entire day.

Overall, Site 2, which had the highest proportion of impervious surfaces, the lowest proportion of total vegetation, and the greatest number of buildings, was consistently the site with the warmest air temperature. This aligns well with the consensus of the literature that local warming is caused by the replacement of vegetation with low albedo impervious surfaces like asphalt and dark colored roofs (eg. EPA, 2008; Giguere, 2012; Lesnikowski, 2014). In fact, in addition to having the highest overall number of buildings, Site 2 also had the greatest proportion of dark colored roofs, at 37%, and the second highest proportion of asphalt, at 27%. Both asphalt and dark roofing material have very low albedos, 0.08 and 0.1, respectively, meaning they absorb most of the solar radiation that they receive rather than reflecting it back into the atmosphere. Once absorbed, these two materials also have fairly high emissivity rates (0.95 and 0.92, respectively), and are therefore quite efficient at emitting heat back to the atmosphere to warm up their surroundings.

It has been noted in past research that the UHI effect is greatest at night, when man-made surface materials that have stored up heat over the course of the day emit that collected heat back into the air in the absence of solar radiation. This process prevents affected areas from cooling overnight as much as they would normally (Jin et al., 2018; Lesnikowski, 2014). The warmer morning air and surface temperature of Site 2 in this study relative to the other sites supported this, suggesting that the dense urban landscape and high number of tall buildings at the site insulated the local atmosphere from normal cooling. Site 2 had the greatest degree of urban morphology and urban canyon effect, as measured by the number of tall buildings, which may have acted to keep the warm air above the site trapped overnight. In comparison, all three of the other sites had a smaller total number of buildings, as well as a smaller number of tall and medium height buildings. Other research also noted the effects of tall buildings on local heat. Two studies identified that temperatures were higher where average building height was greater, noting that this effect was stronger than the effect of vegetation and tree cover in such neighborhoods (Gage & Cooper, 2017; Tian et al., 2019). Site 2 was also farthest away from the coast of the Burrard Inlet, which may have played a role in reduced air flow and nighttime cooling ability compared to the more exposed sites.

As noted in the Results section, Site 2 did not have the warmest surface temperature. In the morning time, Site 4 (Vanier Park) was considerably warmer at the surface than Site 2, and in the afternoon, the surface temperature of Site 2 was lower than both Site 4 and Site 1. The reason for Site 4's warmth is almost certainly due to the need to locate the launch area immediately next to the park on the concrete sidewalk to the west because of RPAS launch restrictions on private property such as public parks. The sidewalk is surrounded by open grass and asphalt roads with no shading from trees and is the most likely cause of the high surface

temperature recorded at this site. Once launched, the drone assembly was moved over the park for the remainder of altitudes.

Despite the warm surface temperature of the Site 4 launch location, once the drone was positioned over the park the air temperature at 20m declined by 2.29°C, making it ultimately lower than the air temperature of Site 2 by 0.39°C. The temperature continued to drop with height up to 40m, where it was 1.06°C cooler than Site 2's equivalent temperature. This lower temperature suggests that the park vegetation has a cooling effect in the air above it, despite the fairly similar proportion of asphalt within the site area (27% at Site 2, and 21% at Site 4). Despite being cooler than Site 2, the park was still warmer overall in the morning than Sites 1 and 3. This temperature difference may be attributable to the relatively high number of low buildings with dark roofs in the adjacent block, in combination with the influence of the inlet on Sites 1 and 3.

The atmosphere above Sites 1 and 3 were the coolest in the morning. Both sites had a relatively similar surface temperature, and exhibited a similar vertical temperature profile in the air above. Both of these sites are located quite close to the inlet and are thus likely to be influenced by the cooling effect of the large adjacent waterbody, whereas Sites 2 and 4 are comparatively more protected. Gage & Cooper (2017) noted a similar cooling effect in locations dominated by water. Ultimately, despite similar exposure to water, Site 3 at the Convention Centre had the coolest morning air temperature of all the sites. This may be attributable to both the proximity to the inlet and the higher proportion of vegetation at this site, including the large expanse of green roof on the nearby Convention Centre and restaurant. It is probable that the higher proportion of vegetation at Site 3, along with the smaller quantity of buildings, aided in radiative and evapotranspirative cooling during the night, leading to a cooler morning temperature.

Vertical temperature profiles of each site changed considerably between the morning and afternoon test flights. As expected, temperatures at all sites warmed by several degrees. In the afternoon, the park at Site 4 appears to have retained its cooling effect in the air above the site. For the same reasons noted earlier, the surface temperature at Site 4 was quite high, but once above the park, the air remained cooler than both Sites 2 and 3. Site 4 remained cooler even at height, whereas Sites 2 and 3 experienced additional warming at higher altitudes compared to the morning. This suggests that the cooling effect of the park is persistent throughout the day, a notion supported by the literature (EPA, 2008; Giguere, 2012; Jin et al., 2018). The air was coolest immediately above the park at an altitude of 20m, after which it warmed slightly but still remained cooler overall.

Site 2 continued to have the warmest temperature overall, however its surface temperature dropped to third place, at 20.66°C. This cooler ground level temperature is likely due to the shading provided by surrounding buildings, a finding supported by other studies (Jin et al. 2018; Tian et al., 2019), and confirmed by recorded visual observations from the site. However, despite the cooler ground surface, the air above Site 2 was quite warm, indicating

that the cooling effect of shading experienced at ground level did not extend up into the UCL and RSL. In fact, the urban warming effect observed at Site 2 appears to have extended all the way up to the maximum measured altitude of 120m. With a calculated UCL height of 22m in this location, this means that the warming effect extended beyond the tallest local buildings and as far up as the uppermost reaches of the RSL (calculated to be 110m). The full extent of the warming effect was not able to be determined however, due to the maximum altitude reached by the RPAS, and was not an objective of this study. The high-altitude extent of warming could be attributable to a number of factors: trapped solar radiation within the urban canyon, anthropogenic heat from energy use and air conditioning released by the surrounding tall buildings throughout the height of the canyon, or the high proportion of man-made, low albedo materials dominating the site. The façade materials of the buildings may have also played a role in heat trapping based on their varying thermal qualities.

Another result of interest from the afternoon test is the change experienced at the Convention Centre (Site 3). Whereas Site 3 had the coolest air temperatures in the morning, by the afternoon this Site's vertical temperature profile had shifted somewhat dramatically to the right, warming by 5.07°C at 20m, and 5.18°C at 40m. This is in contrast to the other sites, which warmed by 1.5-3.5°C at most. Given the higher proportion of vegetation at this site, the presence of the large green roof, and the cooling effects observed in the morning, this result was unexpected. It is possible that the high degree of warming experienced at this site could be a result of a horizontal advection of heat caused by the predominant wind direction. Being a coastal city, summer winds in Vancouver blow predominantly from the west and northwest (Windfinder, 2021), driven by sea breeze circulations. This meteorological phenomenon draws cooler air from the ocean towards the warmer regions over land, an effect that generally becomes more pronounced in the afternoon and early evening (North Carolina Climate Office [NCCO], *n.d.*). A mild westerly wind direction is confirmed by observations recorded at the test sites, though wind data from the Vancouver Harbour CCS weather station did not include wind data to confirm this (see Appendix 1). Based on recorded observations, wind was noted as being quite calm in the morning, but had increased slightly from the west by the afternoon. A westerly wind coming off the ocean would first blow across the warm interior of downtown, gaining heat before blowing across the location of Site 3, which is situated on the easternmost side of the downtown peninsula. This warmer air could then displace any cooled air related to the surface features of Site 3. A similar phenomenon was noted by Pigeon et al. (2007), who observed heat fluxes in a European coastal city during a period of afternoon sea-breezes, and noted that horizontal advection was the dominant process at that time, rather than vertical thermal advection processes.

Two observations support the theory that horizontal advection is causing the increased temperature noted at Site 3. First, Site 3 is located immediately to the east of a section of downtown dominated by high commercial skyscrapers averaging around 80m in height. This matches fairly well with the extent of the warm air column, which reaches up to the 120m mark

and possibly beyond. When wind forces are acting on an urban surface, a plume of warmer air may be advected downwind of the city, which can expand beyond the height of the original layer from which it originates (Zenman, 2012). Figure 11 demonstrates this plume behaviour. Since Site 3 would be receiving mixed warm air from a large extent of downtown, this could explain the height of the warm air observed at this site.

Second, Site 1, which is located on the opposite side of the downtown peninsula, had considerably cooler air temperatures than most of the other sites. Site 1 would be situated in the direct path of the dominant sea breeze, which may explain why the air was so much cooler at this site, despite its higher proportion of impervious surfaces and low proportion of tree canopy coverage. In fact, the afternoon surface temperature of Site 1 was actually the highest of all four sites, which makes sense given its high degree of impermeability and relative lack of shading from trees. Site 1, however, then displayed the greatest drop in temperature between altitudes during an individual launch, dropping from 22.30°C at the surface to 17.92°C at 20m. This could be due to the inflow of ocean air just above the surface which acts to cool the atmosphere considerably. As such, the evidence seems to support the flow of air across the city in a west to east direction.

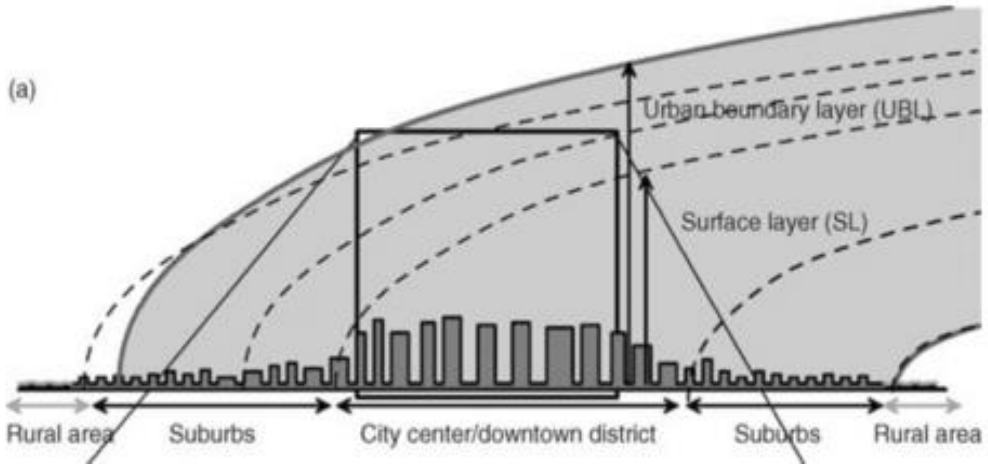

Figure 11: Plume behaviour within the UBL during periods of moderate winds. Reproduced from Zenman (2012)

Interestingly, despite the warmth of the air column, the surface temperature at Site 3 was the coolest of the four sites in the afternoon. It is unlikely that this surface cooling was due to shading from tall buildings, as there are only a few buildings within the site, all of which were far enough away to not provide much shading for the time of day. This may point to the fact that the high proportion of vegetation and the green roof at Site 3 were doing their job of keeping the surface cool, but these actions were overshadowed by the horizontal movement of

the plume overhead. In line with this, green roofs often act to keep the buildings beneath them cool, meaning they require less energy for interior cooling which would be released as anthropogenic heat at ground level outside of the building.

In addition to the local effects at each site discussed above, some general observations for the entire study area were also noted. One of these observations was that air temperatures appeared to converge with increasing altitude in the morning, but not in the afternoon. These observations match well with descriptions of the urban atmosphere provided by Barlow (2014). In the morning, the surface of each site was cooler, therefore the unique warming effect of the local area would be expected to extend only a short distance above it. However, as the surface was progressively heated by solar radiation over the course of the day the vertical extent of warming above the local site would be expected to increase. In either case, once a certain height is reached, local atmospheric forcings become negligible and air temperature should become homogenous due to mixing in the upper reaches of the UBL (Barlow, 2014). This homogeneity was observed at the convergence point in the morning profiles. In the afternoon, however, the reach of the increased warming effects from local features appears to have extended further into the atmosphere, resulting in a divergence of temperatures across sites at higher altitudes.

Finally, it should be noted that all sites except the parking lot exhibited what could be an atmospheric temperature inversion at around 40m. This inversion persisted into the afternoon at Sites 1 and 4, which were the western most sites, but disappeared at Site 3 in the afternoon, potentially overtaken by the horizontal advection processed presumed to be taking place there. Environment Canada did not have historical information available regarding the presence of a frontal inversion over Vancouver at the time of testing to confirm if an inversion was taking place. A frontal inversion caused by the collision of cool ocean air with warmer air over the city (Higgens, 2020) is possible, and would align with the theory for why such a cool layer of air existed at 20m and 40m over Site 1 into the afternoon.

5.2 Winter Vertical Profiles

As noted in the Results section, during the winter test day variation between vertical temperature profiles was much less pronounced. All four sites showed a fairly similar vertical profile in both the morning and afternoon, which was warmest at the surface level and decreased more or less steadily with height. In the morning, Sites 1, 2, and 4 all displayed a similar lapse rate pattern, with Site 4 being the coolest and Site 1 being the warmest. Throughout the entire air column, these three sites varied in temperature by about 0.30 - 0.65°C.

Site 3 exhibited the greatest level of variation from the other three sites in the middle region with a period of steady temperature occurring from 20m to 70m, but otherwise had a similar profile in the lower and upper atmosphere. This could be a result of the eastern exposure of Site 3 to the inlet, which experiences an easterly prevailing wind direction in the

winter. While in the summer wind blows predominantly from the west and northwest off the ocean, in the winter this wind pattern reverses to flow from the east. The ocean's high heat capacity allows it to maintain a relatively stable temperature year-round, while land temperatures drop in the winter (NCCO, *n.d.*). This reversal of temperature gradient causes the wind to flow in the opposite direction. As such, it is possible that Site 3's warmer air in the 40-70m range could have been a result of warm air from the inlet blowing across it.

In the afternoon, all four sites again displayed a fairly similar atmospheric structure. There was a zone of slightly increased variation in temperature between sites from 20m-70m. The upper bounds of the UCL, as determined by the average building height, was calculated to occur within this range at all sites. Therefore, it is possible that this slight variation could simply be due to the zone of increased mixing and turbulence that occurs above the UCL in the upper half of the RSL.

It is possible that the heating properties of the different proportions of surface materials and vegetation at each site were having a minor effect on the air temperature above, even in the winter time. This is evidenced by the fact that Site 2 continued to be on the warmer side, and Site 4 remained on the cooler side. Since the heat capacity of materials is greatly reduced in the winter due to colder ambient temperatures, increased cloud cover and rain interfering with solar radiative gain, it is expected that any UHI effects, if they existed, would be significantly reduced. However, given how small the variations were between the vertical temperature profiles of each site, it is also possible that the observed variations were merely due to random fluctuations and variations in the atmosphere. For this reason, it is not possible to say with certainty that the thermal qualities of local urban features had an impact on temperature variation between sites during the winter season. It is also uncertain whether the UHI effect was present in the study area at all during the winter time. The inclusion of a more distant data point outside of the larger Vancouver metropolitan area may have helped determine if a UHI was present at all, and should be included as a control point in future research.

Some sources of error may have existed during both testing days, but it is expected that they had minimal impact on the results. Firstly, some systematic error may have been introduced by imprecise instrumentation (i.e. the temperature sensors and drones). Due to the format of this experiment and availability of instruments and RPAS, it was not possible to compare the instrumentation used in this study with other instruments to ensure accuracy or precision. However, as a systematic error any imprecision that might exist would be carried through to all of the results and should not influence the temperature variance observed between altitudes or sites. Another possible source of error could arise from the sensor adjustment time at each altitude. This uncertainty was minimized by only considering data after the sensor had been at the intended altitude for 2.5 minutes. This allowed for the two minute adjustment time noted by the sensor manufacturer, plus a safety margin. Lastly, some error may have been introduced due to time delays between launches at some of the sites. For example, in the winter, flights at Site 3 had to be staggered due to a malfunction with one of

the drone sensors that prevented the flight from being controlled in a safe manner. In this case, the first two altitudes were flown as planned, and then the drone was landed and the sensor apparatus and battery were switched before completing a second flight at the other two altitudes. For this reason, flight times were not simultaneous but occurred approximately 24 minutes apart. Small changes in temperatures may have occurred during the time taken to change out the sensor and battery, however, it is not believed that temperatures would have changed significantly enough during that time to impact results

5.3 Regional and Municipal Strategy and Eco-Cities Context

Ecocity Builders define cities as urban eco-systems, analogous in many ways to living, breathing organisms (Ecocity Builders, 2020). Cities are complex, dynamic, constantly changing entities that have numerous inflows and outflows of energy and materials. Cities respond and adapt to their surroundings and the people, materials, and natural systems contained within them. The urban heat island phenomenon is the perfect example of how the complex interplay of energy and materials within a city can result in adverse consequences such as heat breakaway cycles, exacerbation of climate change, and increased exposure of vulnerable populations to heat stress. Understanding and monitoring the material and energy inputs linked to UHIs is therefore important to managing the health of our cities.

Ecocity Builders have created the International Ecocity Framework & Standards (Ecocity Builders, 2021) to guide cities in taking a holistic approach to becoming sustainable urban organisms that can exist and thrive within the bounds of the planet. The framework includes 18 interconnected standards for municipalities to strive towards. Of these 18 standards, three in particular have special relevance for UHI mitigation planning. First is the standard for clean air. The clean air standard highlights the importance of air flow within the local airshed, and speaks to the impact of topographical and urban features on the movement of air and pollutants. The impact of greenhouse gases and climate change is also of importance to this standard. The UHI is a known contributor to climate change, and has a major influence on the air quality of cities. Heat exacerbates photochemical smog production, and urban roughness features interact with weather and surface heat fluxes to influence the movement of pollutants through city neighborhoods. Controlling urban heat can decrease the severity of air pollution and smog. The protection and enhancement of urban forests and the encouragement of green infrastructure like green roofs and walls plays an important role in heat mitigation and climate change resilience. Such features protect residents from heat waves, purify the air, and make neighborhoods more pleasant. Focusing greening efforts on vulnerable neighbourhoods with higher proportions of dense buildings, dark roofs, and impermeable surfaces should be a priority.

The second Ecocity strategy most closely tied to UHI management is the standard for green buildings. Buildings are an integral part of the urban eco-system, and should be designed as holistic systems that integrate seamlessly with their natural surroundings (Ecocity Builders, 2021). Buildings should leverage the services provided by nature (eg. solar radiation and

thermal mass, shading from trees, and natural airflow and ventilation) and work with the natural materials and energy flows of their surroundings to maximize efficiency and reduce energy needs. All of these strategies for building design complement UHI management strategies, and can be used together to reduce the thermal impact of buildings. Buildings should be oriented in space to maximize airflow and natural ventilation. Exterior materials should be chosen with high albedo and low capacity for thermal gain, especially on roofs, and should leverage shading from trees whenever possible. Green roofs and walls should be encouraged and maybe even incentivized. Further, buildings must be airtight to prevent heating and cooling loss, which will reduce the energy demand of buildings and thus their anthropogenic heat production.

Finally, the Ecocity standard for access by proximity is also related to UHI mitigation, though less directly than the preceding standards. Access by proximity is an important umbrella goal for green cities because it also supports many of the other standards (Ecocity Builders, 2021). When cities are designed for easy access to essential services without the use of vehicles, cities also benefit from reduced GHG emissions, cleaner air and water, improved access to food, better quality of life for residents, and healthy local economies. Access by proximity acts to reduce UHI impacts by encouraging more pedestrian and bike friendly transport, which typically results in the planting of more vegetation and trees for pedestrian enjoyment. Pedestrian based design also reduces the need for large swaths of asphalt street and is better suited for the use of pervious surfaces since they don't need to support the weight of multiple heavy vehicles. This improves the health of local soils and encourages the growth of the urban forest. An increase in the proportion of vegetation and a decrease in the proportion of impervious surfaces is an important protective measure against UHI formation (Giguere, 2012; City of Vancouver and Vancouver Park Board, 2019).

The results of this study help to demonstrate the influence of local microscale features on atmospheric heat responses within cities. When localized impacts are better understood, problem areas can be more easily identified and addressed at the community scale. Since UHI's are ultimately caused by local urban features, community scale approaches allow for the customization needed in addressing urban heat problems. Addressing urban heat problems is important for ensuring a healthy, functioning ecocity that does not harm the planet. Some major takeaways from this study that can be applied on the community scale include:

<u>Influence of Buildings</u>

- A higher building density, especially the presence of more tall and medium sized buildings, is correlated with warmer local air temperatures. The prevalence of dark colored roofs also plays a role
- Highly urban areas with large proportions of buildings and impervious surfaces may be cooler at the ground level due to shading from buildings, but this shading effect does not keep the air above cool. The heat above such locations may extend beyond the UCL and into the upper reaches of the RSL

- The surfaces of building facades in urban canyons, as well as anthropogenic heat produced by tall buildings, may contribute to the column of warm air above dense urban areas.
    - Further research on this impact would be beneficial to shed more light on the impact of building materials and anthropogenic heat from tall buildings on the upper layers of the UCL/RSL

Urban Greening

- Greener sites, such as the site with a local park, experienced cooling at height which persisted throughout the heat of the afternoon, compared to sites with a higher proportion of impervious surfaces

Horizontal Advection

- Horizontal advection of heat and pollutants due to sea-breezes is a factor that should be considered in heat mitigation planning in coastal cities like Vancouver
- Green roofs likely provide cooling effects at the ground level, but this cooling effect on the atmosphere above neighbourhoods may be overshadowed by horizontal advection forces for areas downwind of a large urban area
- The widespread application of mitigating features across most or all of an urban landscape may help to prevent heat and pollution spread due to horizontal advection

A review of the City of Vancouver's strategies and frameworks related to climate change adaptation revealed that the City is addressing many of the Ecocity strategies in their plans for the future. Vancouver's Greenest City Action Plan (2015) targets 10 goals which are well aligned with many of the Ecocity standards. Of relevance to UHI management are the goals related to Green Buildings, Access to Nature, Clean Air, and Green Transportation. The City intends to improve the proportion of tree canopy coverage from the 2013 average of 18% up to 22% by 2050. Additionally, the City intends to add more green spaces and ensure that all citizens have access to a city park within a 5 minute walk from their residence. To compliment the Greenest City Action Plan, Vancouver has a comprehensive Urban Forest Strategy (2018) which aims to protect and promote the growth of the urban forest. This document catalogues the health and coverage of the urban forest, and also documents the prevalence of impervious surfaces within the city, with the goal of targeting vulnerable neighborhoods which could benefit most from the heat mitigation provided by more urban trees. Despite this robust strategy, the document mentions green infrastructure only once, and does not mention green roofs or walls at all. A greater emphasis on increasing adoption of green roofs and walls within city infrastructure would be of benefit to the city. A more aggressive target of 25% urban forest coverage by 2050 would also be beneficial.

Vancouver's Greenest City Action Plan also has a Green Building Goal. This goal focuses primarily on decreasing the energy use of buildings to help reduce emissions from fossil fuels, as building energy use makes up 64% of all energy use within the City (City of Vancouver, 2015). The energy efficiency of buildings is an important goal that has implications on the UHI. More efficient buildings produce less anthropogenic heat, which is especially important for climate change resiliency. However, the plan does not mention the role of dark colored roofs, or the thermal properties of building materials such as albedo and emissivity. Consideration of such features will play a role in energy efficiency by reducing the solar gain of buildings and thus the thermal load of building interiors. Importantly, these features will also have a beneficial impact on the outdoor environment through the mitigation of UHIs. As such, the City should highlight these building features as important considerations in the goal to achieve greener, ecocity standard buildings, and should include them in both their new building and retrofitting policies.

Lastly, a review of Metro Vancouver's Climate 2050 Framework (2019) was undertaken. This framework proved to be very robust with regards to the importance of mitigating UHI to ensure a climate resilient region. The region's framework speaks repeatedly to the expected rise in temperatures and the risk it poses to the population at large, especially vulnerable groups. The importance of vegetation, trees, and parks for their multiple ecosystem services is highlighted: rainwater collection and flood control, local cooling, building shading for reducing energy demand, biodiversity support, and resident comfort and well-being. Bioswales, green roofs, and other green infrastructure are all listed as important features for increasing resilience. Similar to the City of Vancouver's Urban Forest Strategy, Metro Vancouver states their intent to prioritize the greening of higher risk neighbourhoods to better balance the greater impact of climate change felt by vulnerable populations. The region also has a plan for driving better building design, and notes that government, utilities, and building owners must consider the issues of increasing heat into building design and modify their policies and planning to better accommodate these changes. All of this should be considered in the context of careful design and land use for the growing region, to encourage access by proximity and the associated benefits it brings when working towards becoming an ecocity.

6.0 Conclusion

The efforts of this study enabled the measurement and comparison of vertical air temperature profiles in downtown Vancouver for the first time. The study findings were able to corroborate the results of similar studies that analysed surface temperatures in urban landscapes, as well as identifying some new evidence. For example, results verified that high degrees of vegetation and tree canopy coverage such as urban parks have protective cooling effects, and that areas with greater degrees of impervious surfaces are warmer. Study results also supported theories about the impact of tall buildings on heat: specifically, that tall buildings likely insulate interior locations from normal cooling overnight, and that daytime

surface temperatures in areas with greater urban canyons are cooler. However, this study also noted that the trapped air within urban canyons remains warm into the morning even at height, and that the daytime cooling effect noted at the surface of such locations does not extend into the air above. This warm column of air appeared to extend far up into the RSL, beyond the average building height and the height of the tallest local buildings.

Another finding of note is the possible significance of horizontal advection due to coastal sea breezes in heat distribution. One site studied, which was located next to several heat mitigating features such as a large green roof, a small urban park, and the ocean, was coolest in the morning but exhibited significant warming during the afternoon, against expectations. Dominant sea breeze directions in the region however may have blown warm air from the adjacent downtown core over the site, dominating the heat mitigating features of the site. This also speaks to the importance of having UHI mitigation features integrated across the entire downtown, as isolated mitigation features may not have enough of an impact.

In summary, an improved understanding of the impact of local features on both surface temperatures and the air temperatures above will better inform UHI mitigation strategies. Mitigation strategies must be applied at the local and community scale, as well as the municipal and regional scale, in order to have a meaningful impact on improving city health and resiliency to climate change. The International Ecocity Framework & Standards provides a robust framework for the holistic application of lessons learned from UHI focused research studies such as this one. Additionally, further research to observe vertical temperature profiles in a variety of urban locations, away from areas influenced by the ocean, would be beneficial to better understand the impact of urban features on local atmospheric heat. The City of Vancouver and the larger Metro Vancouver region have made significant steps towards identifying and addressing the issue of UHIs within the Ecocity framework. However, additional emphasis on the importance of building material selection, reduction of dark roofs, and more green infrastructure could further improve the robustness of their strategies for managing urban heat.

7.0 References

Adkins, K., Wambolt, P., Sescu, A., Swinford, C., Macchiarella, N. (2020). Observational Practices for Urban Microclimates Using Meteorologically Instrumented Unmanned Aircraft Systems. *Atmosphere, 11*(9), 1008. https://doi.org/10.3390/atmos11091008

Akbari, H., Konopacki, S. (1998). The impact of reflectivity and emissivity of roofs on building cooling and heating energy use. *Proceedings of Thermal VII: Thermal Performance of the Exterior Envelopes of Buildings VII, December, 1998.* American Society of Heating, Refrigeration, and Air-Conditioning Engineers, Inc.

Arnfield, A. (2003). Two decades of urban climate research: a review of turbulence, exchanges of energy and water, and the urban heat island*. International Journal of Climatology. 23* (1), 1–26. http://dx.doi.org/10.1002/joc.859

Barlow, J. (2014). Progress in observing and modelling the urban boundary layer. *Urban Climate, 10*. 216-240. doi: http://dx.doi.org/10.1016/j.uclim.2014.03.011

City of Vancouver. (2015). Greenest City 2020 Action Plan, Part Two: 2015-2020. Retrieved from: https://vancouver.ca/green-vancouver/greenest-city-action-plan.aspx

City of Vancouver. (2021). Zoning and Land Use Document Library. Retrieved from: https://vancouver.ca/home-property-development/zoning-and-land-use-policies-document-library.aspx#regulation-zoning-regulations

City of Vancouver and Vancouver Park Board. (2018). Urban Forest Strategy: 2018 Update. Retrieved from: https://vancouver.ca/home-property-development/urban-forest-strategy.aspx

Dias, N., Goncalves, J., Freire, L., Hasegawa, T., Malheiros, A. (2012). Obtaining Potential Virtual Temperature Profiles, Entrainment Fluxes, and Spectra from Mini Unmanned Aerial Vehicle Data. *Boundary Layer Meteorology, 145*. 93-111. Doi: 10.1007/s10546-011-9693-2

Ecocity Builders (2020). What is an Ecocity?. Retrieved from: https://ecocitybuilders.org/what-is-an-ecocity/

Ecocity Builders. (2021). Ecocity Standards – an Initiative of Ecocity Builders. Retrieved from: https://ecocitystandards.org/

Engineering ToolBox. (2003). Heat Capacity. [online]. Retrieved from: https://www.engineeringtoolbox.com/heat-capacity-d_338.html

Environment Canada. (2020). Almanac Averages and Extremes. Retrieved from: https://climate.weather.gc.ca/climate_data/almanac_selection_e.html

Environment Canada. (2021). Historical Data. Retrieved from: https://climate.weather.gc.ca/historical_data/search_historic_data_e.html

Gage, E., Cooper, D. (2017). Relationships between landscape pattern metrics, vertical structure and surface urban Heat Island formation in a Colorado suburb. *Urban Ecosystems, 20*. 1229-1238. doi: 10.1007/s11252-017-0675-0

Giguere, M. (2012). Urban Heat Island Mitigation Strategies: a Literature Review. Institut National de Sante Publique Quebec. Retrieved from: https://www.inspq.qc.ca/pdf/publications/1513_UrbanHeatIslandMitigationStrategies.pdf

Gorlach, I.A., Kislov, A.V., Alekseeva. (2018). Experience of Studying the Vertical Structure of an Urban Heat Island Based on Satellite Data. Atmospheric and Oceanic Physics, 54(9), 37-46. Retrieved from: https://search.proquest.com/docview/2383069092?accountid=26389&pq-origsite=summon

Health Canada. (2009, November 30). Climate Change and Health—Adaptation Bulletin. The Urban Heat Island Effect: Causes, Health Impacts and Mitigation Strategies. Number 1, ISSN: 1920-2687. Government of Canada. https://www.canada.ca/en/health-canada/services/environmental-workplace-health/reports-publications/climate-change-health/climate-change-health-adaptation-bulletin-number-1-november-2009-revised-december-2010-health-canada-2009.html

Higgins, J. (2020). Temperature Inversion. *Encyclopaedia Brittanica.* Retrieved from: https://www.britannica.com/science/temperature-inversion

Intergovernmental Panel on Climate Change. (2019). Special Report: Climate Change and Land. Chapter 2, Land-Climate Interactions. Retrieved from: https://www.ipcc.ch/srccl/chapter/chapter-2/

Jin, H., Cui, P., Wong, N. H., & Ignatius, M. (2018). Assessing the Effects of Urban Morphology Parameters on Microclimate in Singapore to Control the Urban Heat Island Effect. Sustainability, 10(1), 206. http://dx.doi.org/10.3390/su10010206

Kroonenberg, A. C., Martin, S., Beyrich, F. Bange, J. (2012). Spatially-Averaged Temperature Structure Parameter Over a Heterogenous Surface Measured by an Unmanned Aerial Vehicle. *Boundary Layer Meteorol, 142,* 55-77. doi: 10.1007/s10546-011-9662-9

Lesnikowski, A. (2014). Adaptation to Urban Heat Island Effect in Vancouver, BC: A case study in analyzing vulnerability and adaptation opportunities. University of British Columbia: SCARP

Graduating Projects. Retrieved from: https://open.library.ubc.ca/cIRcle/collections/graduateresearch/310/items/1.0075852

Lokoshchenko, M., Korneva, I., Kochin, A., Dubovetsky, A., Novitsky, M., Razin, P. (2016). Vertical Extension of the Urban Heat Island above Moscow. Doklady Earth Sciences, 466(1), 70-74. Retrieved from: https://search.proquest.com/docview/1771303072?pq-origsite=summon&accountid=26389

Martin, S., Beyrich, F., Bange, J. (2014). Observing Entrainment Processes Using a Small Unmanned Aerial Vehicle: A Feasibility Study. Boundary Layer Meteorology, 150. 449-467. doi: 10.1007/s10546-013-9880-4

Masic, A., Bibic, D., Pikula, B., Dzaferovic-Masic, E., Musemic, R. (2019). Experimental Study of Temperature Inversions Above Urban Area Using Unmanned Aerial Vehicle. *Thermal Science, 23*(6A). 3327-3338. doi: https://doi.org/10.2298/TSCI180227250M

Metro Vancouver. (2016). Climate Projections for Metro Vancouver. Retrieved from: http://www.metrovancouver.org/services/air-quality/AirQualityPublications/ClimateProjectionsForMetroVancouver.pdf

Metro Vancouver. (2019). Climate 2050 Strategic Framework. Retrieved from: http://www.metrovancouver.org/services/air-quality/climate-action/climate2050/about/climate-2050/Pages/default.aspx

North Carolina Climate Office. (no date). Sea and Land Breezes. Retrieved from: https://climate.ncsu.edu/edu/Breezes

Pigeon, G. Lemonsu, A., Grimmond, C., Durand, P., Thouron, O., Masson, M. (2007). Divergence of turbulent fluxes in the surface layer: case of a coastal city. *Boundary-Layer Meteorology, 124*(2). 269-290. Doi: 10.1007/s10546-007-9160-2

Salata, F., Golasi, I., Petitti, D., de Lieto Vollaro, E., Coppi, M., de Lieto Vollaro, A. (2017) Relating microclimate, human thermal comfort and health during heat waves: An analysis of heat island mitigation strategies through a case study in an urban outdoor environment. *Sustainable Cities and Society, 30.* 79-96. doi: http://dx.doi.org/10.1016/j.scs.2017.01.006

Sugawara, H., Narita, K., Mikami, T. (2021). Vertical structure of the cool island in a large urban park. *Urban Climate, 35.* 100744. doi: https://doi.org/10.1016/j.uclim.2020.100744

Tian, Y., Zhou, W. Qian, Y., Zheng, Z., Yan, J. (2019). The effect of urban 2D and 3D morphology on air temperature in residential neighborhoods. *Landscape Ecology, 34*. 1161-1178.doi: https://doi.org/10.1007/s10980-019-00834-7(0123456789().,-volV() 0123458697().,-volV)

US Environmental Protection Agency. (2008). Reducing urban heat islands: Compendium of strategies [Reports and Assessments]. US EPA. https://www.epa.gov/heatislands/heat-island-compendium

Wang, M., Zhang, X., Yan, X. (2013). Modeling the climatic effects of urbanization in the Beijing–Tianjin–Hebei metropolitan area. *Theoretical Applied Climatology, 113.* 377-385. doi: 10.1007/s00704-012-0790-z

Windfinder. (2021). False Creek Fuels Wind and Weather Statistics. Retrieved from: https://www.windfinder.com/windstatistics/false_creek_fuels_vancouver

Voogt, J. (2017). How Researchers Measure Urban Heat Islands [Lecture slides]. University of Western Ontario. https://19january2017snapshot.epa.gov/sites/production/files/2014-07/documents/epa_how_to_measure_a_uhi.pdf

Yu, S., Chen, Z., Yu, B., Wang, L., Wu, B., Wu, J, Zhao, F. (2020). Exploring the relationship between 2D/3D landscape pattern and land surface temperature based on explainable eXtreme Gradient Boosting tree: A case study of Shanghai, China. *Science of the Total Environment, 725.* 138229. Doi: https://doi.org/10.1016/j.scitotenv.2020.138229

Zeman, F. (Ed.). (2012). Metropolitan Sustainability [ebook]. Cambridge, UK: Woodhead Publishing.

Appendices

Appendix 1: Environment Canada Weather Station Data – Vancouver Harbour CCS

Source: Environment Canada. (2021). Historical Data. Retrieved from: https://climate.weather.gc.ca/historical_data/search_historic_data_e.html

September 30, 2020 (from hourly data report)

Time	Temp (°C)	Dew Point (°C)	Rel. Humidity (%)	Precip. (mm)	Wind Dir. (10s of °)	Wind Speed (km/h)
10:00am	16.7	12.8	78	0	NA	NA
3:00pm	20.4	12.6	63	0	NA	NA

*NA – not available

January 29, 2021 (from hourly data report)

Time	Temp (°C)	Dew Point (°C)	Rel. Humidity (%)	Precip. (mm)	Wind Dir. (10s of °)	Wind Speed (km/h)
10:00am	5.6	4.2	90	0	NA	NA
3:00pm	7.5	2.5	70	0	NA	NA

Appendix 2: Example Raw Data from Several Altitudes

Site 1, Drone 1, data collected at ground level, 20m and 40m – Sep 30, 2020, morning launch

- Shaded yellow boxes indicate range where temperature was averaged

Location #	Site 1, drone 1 (S1.D1) Date Time, GMT-07:00		Temp, °C (T_ext)	
41	09/30/20 09:50:00 A	9:50:00 AM	17.653	Test Start, ground, 1m
42	09/30/20 09:50:30 A	9:50:30 AM	17.629	
43	09/30/20 09:51:00 AI	9:51:00 AM	17.582	
44	09/30/20 09:51:30 AI	9:51:30 AM	17.51	
45	09/30/20 09:52:00 A	9:52:00 AM	17.486	
46	09/30/20 09:52:30 A	9:52:30 AM	17.439	
47	09/30/20 09:53:00 A	9:53:00 AM	17.391	
48	09/30/20 09:53:30 A	9:53:30 AM	17.344	
49	09/30/20 09:54:00 A	9:54:00 AM	17.296	
50	09/30/20 09:54:30 A	9:54:30 AM	17.296	
51	09/30/20 09:55:00 A	9:55:00 AM	17.344	
52	09/30/20 09:55:30 A	9:55:30 AM	17.391	
53	09/30/20 09:56:00 A	9:56:00 AM	17.439	
54	09/30/20 09:56:30 A	9:56:30 AM	17.439	
55	09/30/20 09:57:00 A	9:57:00 AM	17.391	
56	09/30/20 09:57:30 A	9:57:30 AM	17.368	
57	09/30/20 09:58:00 A	9:58:00 AM	17.32	
58	09/30/20 09:58:30 A	9:58:30 AM	17.249	
59	09/30/20 09:59:00 A	9:59:00 AM	17.058	
60	09/30/20 09:59:30 A	9:59:30 AM	16.415	Launch to 40m
61	09/30/20 10:00:00 AI	10:00:00 AM	16.225	
62	09/30/20 10:00:30 AI	10:00:30 AM	16.129	
63	09/30/20 10:01:00 AM	10:01:00 AM	16.082	
64	09/30/20 10:01:30 AM	10:01:30 AM	16.034	
65	09/30/20 10:02:00 AI	10:02:00 AM	16.034	
66	09/30/20 10:02:30 AI	10:02:30 AM	16.058	
67	09/30/20 10:03:00 AI	10:03:00 AM	16.106	
68	09/30/20 10:03:30 AI	10:03:30 AM	16.106	
69	09/30/20 10:04:00 AI	10:04:00 AM	16.129	
70	09/30/20 10:04:30 AI	10:04:30 AM	16.153	
71	09/30/20 10:05:00 AI	10:05:00 AM	16.296	
72	09/30/20 10:05:30 AI	10:05:30 AM	16.439	
73	09/30/20 10:06:00 AI	10:06:00 AM	16.558	
74	09/30/20 10:06:30 AI	10:06:30 AM	16.606	
75	09/30/20 10:07:00 AI	10:07:00 AM	16.63	
76	09/30/20 10:07:30 AI	10:07:30 AM	16.654	Change to 20m
77	09/30/20 10:08:00 AI	10:08:00 AM	16.606	
78	09/30/20 10:08:30 AI	10:08:30 AM	16.392	
79	09/30/20 10:09:00 AI	10:09:00 AM	16.32	
80	09/30/20 10:09:30 AI	10:09:30 AM	16.32	
81	09/30/20 10:10:00 AM	10:10:00 AM	16.32	
82	09/30/20 10:10:30 AM	10:10:30 AM	16.296	
83	09/30/20 10:11:00 AM	10:11:00 AM	16.296	
84	09/30/20 10:11:30 AM	10:11:30 AM	16.32	
85	09/30/20 10:12:00 AM	10:12:00 AM	16.344	
86	09/30/20 10:12:30 AM	10:12:30 AM	16.344	
87	09/30/20 10:13:00 AM	10:13:00 AM	16.344	
88	09/30/20 10:13:30 AM	10:13:30 AM	16.344	
89	09/30/20 10:14:00 AM	10:14:00 AM	16.344	
90	09/30/20 10:14:30 AM	10:14:30 AM	16.32	
91	09/30/20 10:15:00 AM	10:15:00 AM	16.225	
92	09/30/20 10:15:30 AM	10:15:30 AM	16.177	
93	09/30/20 10:16:00 AM	10:16:00 AM	16.201	
94	09/30/20 10:16:30 AM		16.153	End of test, land

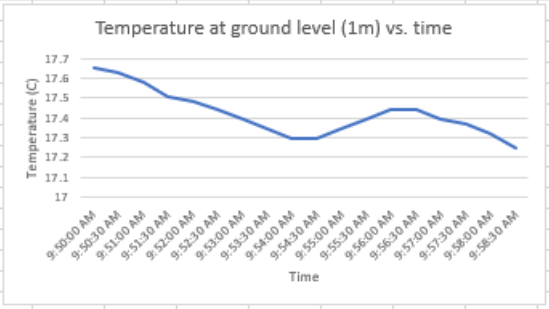

Average temp at atlitude
17.37

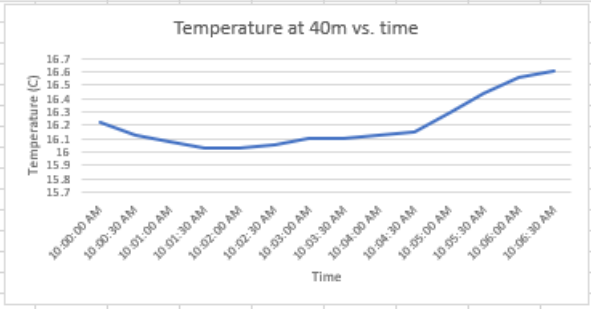

Average temp at atlitude
16.2088

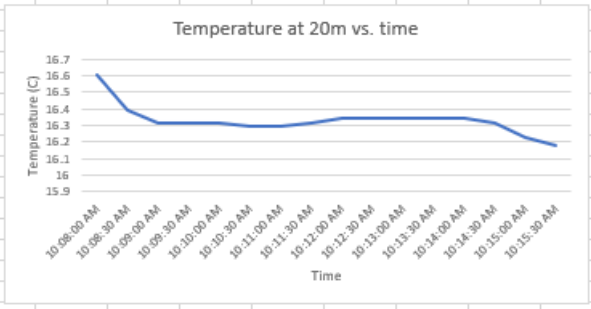

Average temp at atlitude
16.3179

Site 3, Drone 1, data collected at ground level, 20m and 40m – January 29, 2021, afternoon launch

- Shaded yellow boxes indicate range where temperature was averaged

Location #	Site 3, drone 1(S3.D1) Date Time, GMT-08:00		Temp, °C (T_ext)	
642	01/29/2102:50:30 PM	2:50:30 PM	7.745	Start test, ground level, 1m
643	01/29/2102:51:00 PM	2:51:00 PM	7.745	
644	01/29/2102:51:30 PM	2:51:30 PM	7.745	
645	01/29/2102:52:00 PM	2:52:00 PM	7.77	
646	01/29/2102:52:30 PM	2:52:30 PM	7.82	
647	01/29/2102:53:00 PM	2:53:00 PM	7.845	
648	01/29/2102:53:30 PM	2:53:30 PM	7.895	
649	01/29/2102:54:00 PM	2:54:00 PM	7.895	
650	01/29/2102:54:30 PM	2:54:30 PM	7.895	
651	01/29/2102:55:00 PM	2:55:00 PM	7.87	
652	01/29/2102:55:30 PM	2:55:30 PM	7.895	
653	01/29/2102:56:00 PM	2:56:00 PM	7.895	
654	01/29/2102:56:30 PM	2:56:30 PM	7.92	
655	01/29/2102:57:00 PM	2:57:00 PM	7.895	
656	01/29/2102:57:30 PM	2:57:30 PM	7.92	
657	01/29/2102:58:00 PM	2:58:00 PM	7.945	
658	01/29/2102:58:30 PM	2:58:30 PM	7.97	
659	01/29/2102:59:00 PM	2:59:00 PM	7.92	
660	01/29/2102:59:30 PM	2:59:30 PM	7.795	
661	01/29/2103:00:00 PM	3:00:00 PM	7.619	Launch to 20m
662	01/29/2103:00:30 PM	3:00:30 PM	7.494	
663	01/29/2103:01:00 PM	3:01:00 PM	7.368	
664	01/29/2103:01:30 PM	3:01:30 PM	7.343	
665	01/29/2103:02:00 PM	3:02:00 PM	7.318	
666	01/29/2103:02:30 PM	3:02:30 PM	7.268	
667	01/29/2103:03:00 PM	3:03:00 PM	7.268	
668	01/29/2103:03:30 PM	3:03:30 PM	7.268	
669	01/29/2103:04:00 PM	3:04:00 PM	7.293	
670	01/29/2103:04:30 PM	3:04:30 PM	7.268	
671	01/29/2103:05:00 PM	3:05:00 PM	7.268	
672	01/29/2103:05:30 PM	3:05:30 PM	7.268	
673	01/29/2103:06:00 PM	3:06:00 PM	7.293	
674	01/29/2103:06:30 PM	3:06:30 PM	7.293	
675	01/29/2103:07:00 PM	3:07:00 PM	7.343	
676	01/29/2103:07:30 PM	3:07:30 PM	7.318	
677	01/29/2103:08:00 PM	3:08:00 PM	7.293	
678	01/29/2103:08:30 PM	3:08:30 PM	7.242	Change to 40m
679	01/29/2103:09:00 PM	3:09:00 PM	7.167	
680	01/29/2103:09:30 PM	3:09:30 PM	7.192	
681	01/29/2103:10:00 PM	3:10:00 PM	7.192	
682	01/29/2103:10:30 PM	3:10:30 PM	7.192	
683	01/29/2103:11:00 PM	3:11:00 PM	7.167	
684	01/29/2103:11:30 PM	3:11:30 PM	7.142	
685	01/29/2103:12:00 PM	3:12:00 PM	7.142	
686	01/29/2103:12:30 PM	3:12:30 PM	7.142	
687	01/29/2103:13:00 PM	3:13:00 PM	7.192	
688	01/29/2103:13:30 PM	3:13:30 PM	7.217	
689	01/29/2103:14:00 PM	3:14:00 PM	7.217	
690	01/29/2103:14:30 PM	3:14:30 PM	7.217	
691	01/29/2103:15:00 PM	3:15:00 PM	7.217	
692	01/29/2103:15:30 PM	3:15:30 PM	7.217	
693	01/29/2103:16:00 PM	3:16:00 PM	7.192	
694	01/29/2103:16:30 PM		7.217	End test, land

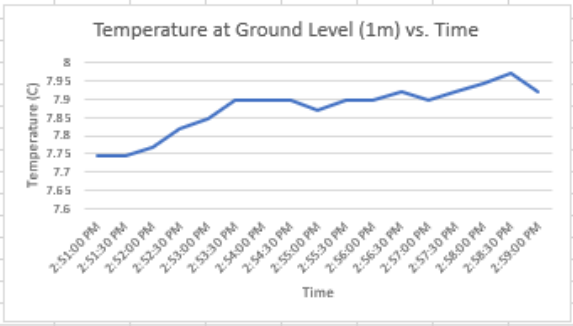

Average temp at 7.91

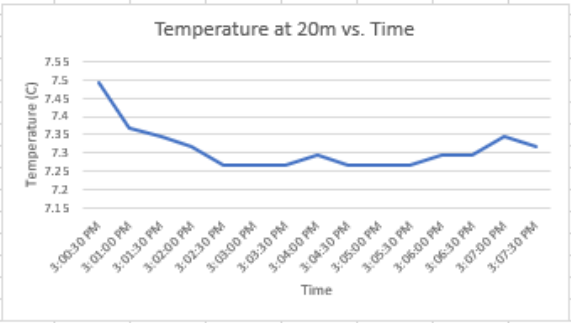

Average temp at 7.283

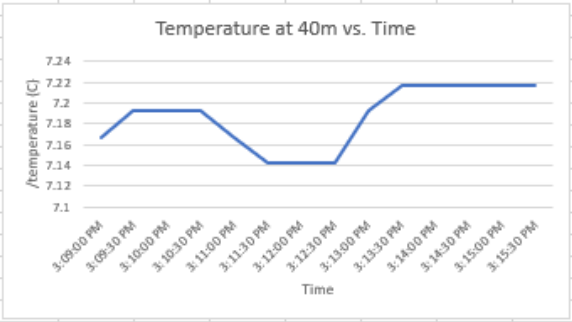

Average temp at 7.1837

Appendix 3: Independent Vertical Temperature Profile Graphs with DALR and MALR

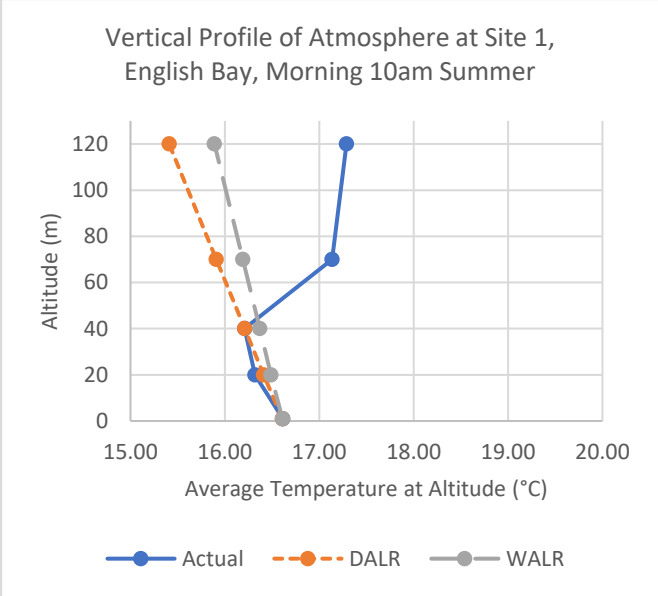

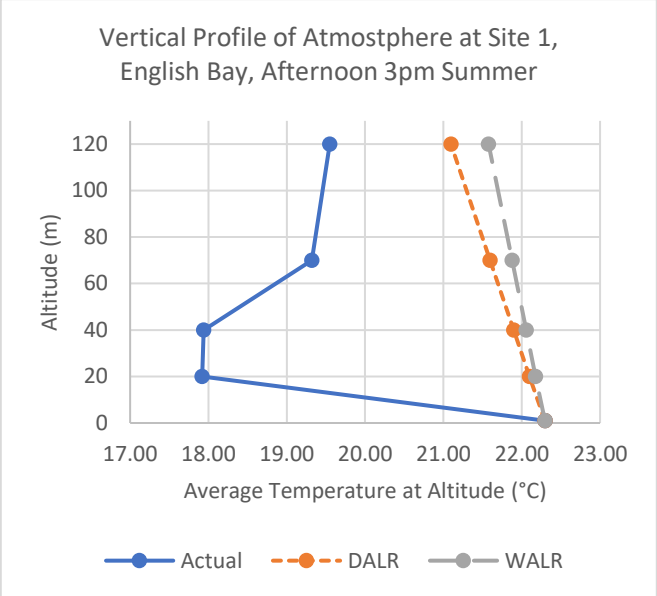

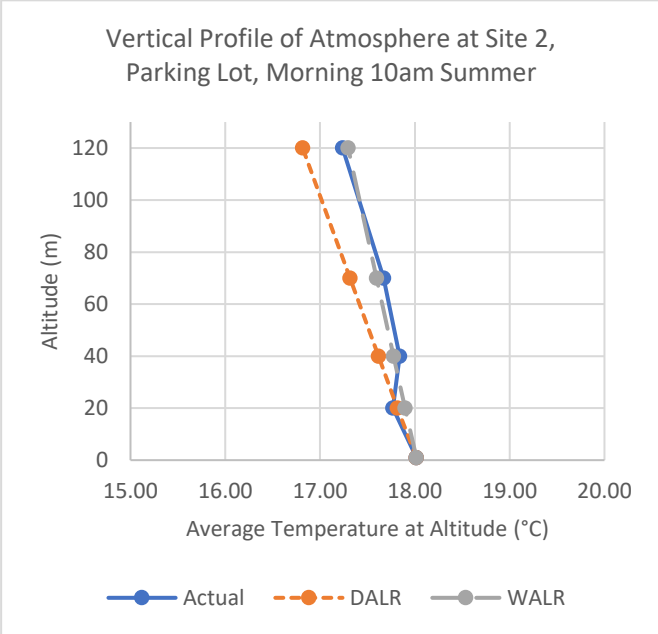

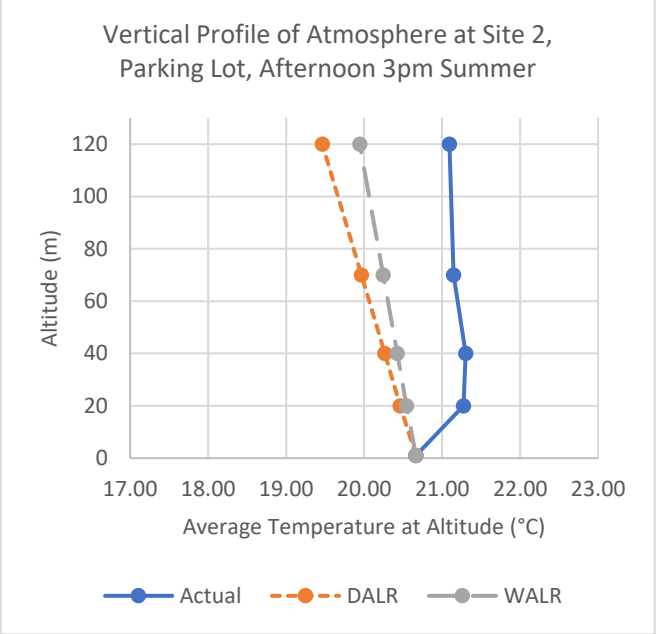

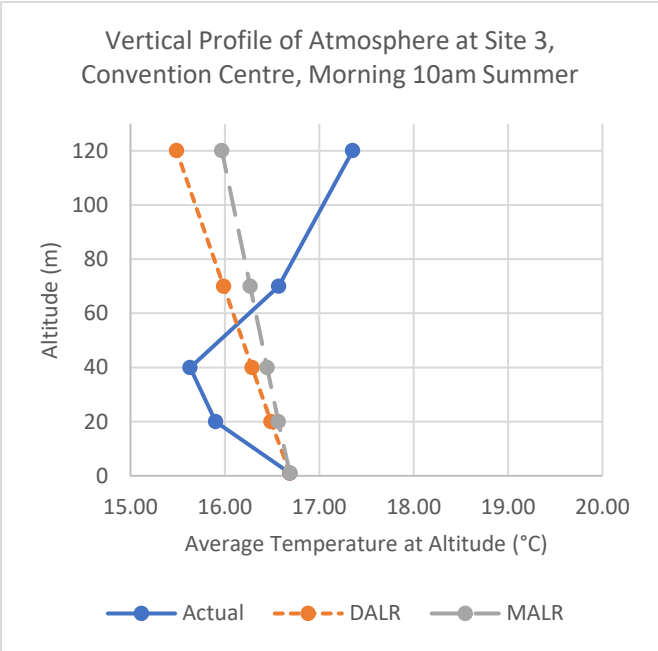
Vertical Profile of Atmosphere at Site 3, Convention Centre, Morning 10am Summer
Altitude (m)
120
100
80
60
40
20
0
15.00
16.00
17.00
18.00
19.00
20.00
Average Temperature at Altitude (°C)
Actual
DALR
MALR

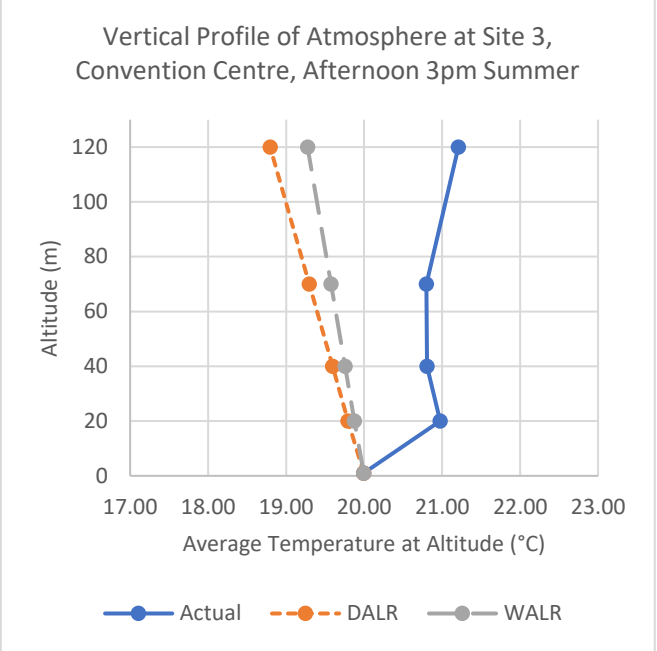
Vertical Profile of Atmosphere at Site 3, Convention Centre, Afternoon 3pm Summer
Altitude (m)
120
100
80
60
40
20
0
17.00
18.00
19.00
20.00
21.00
22.00
23.00
Average Temperature at Altitude (°C)
Actual
DALR
WALR

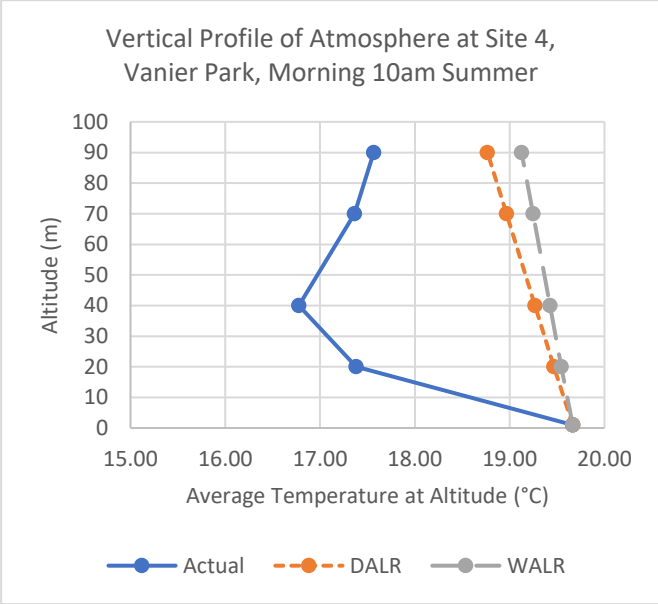
Vertical Profile of Atmosphere at Site 4, Vanier Park, Morning 10am Summer
Altitude (m)
100
90
80
70
60
50
40
30
20
10
0
15.00
16.00
17.00
18.00
19.00
20.00
Average Temperature at Altitude (°C)
Actual
DALR
WALR

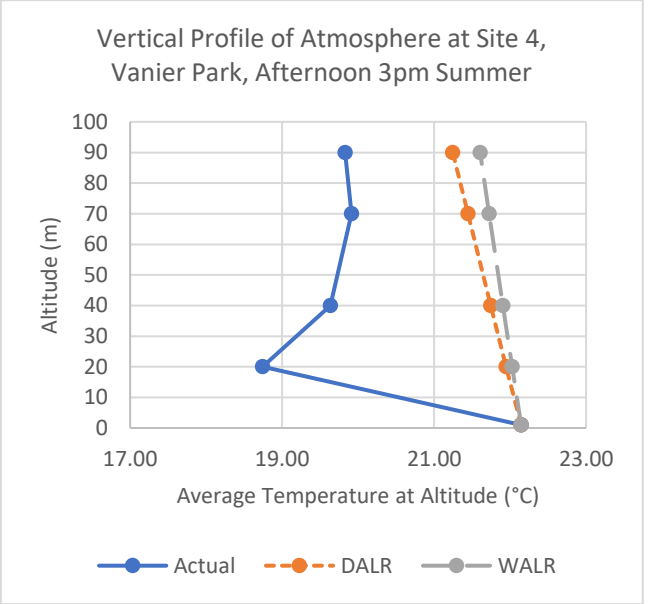
Vertical Profile of Atmosphere at Site 4, Vanier Park, Afternoon 3pm Summer
Altitude (m)
100
90
80
70
60
50
40
30
20
10
0
17.00
19.00
21.00
23.00
Average Temperature at Altitude (°C)
Actual
DALR
WALR

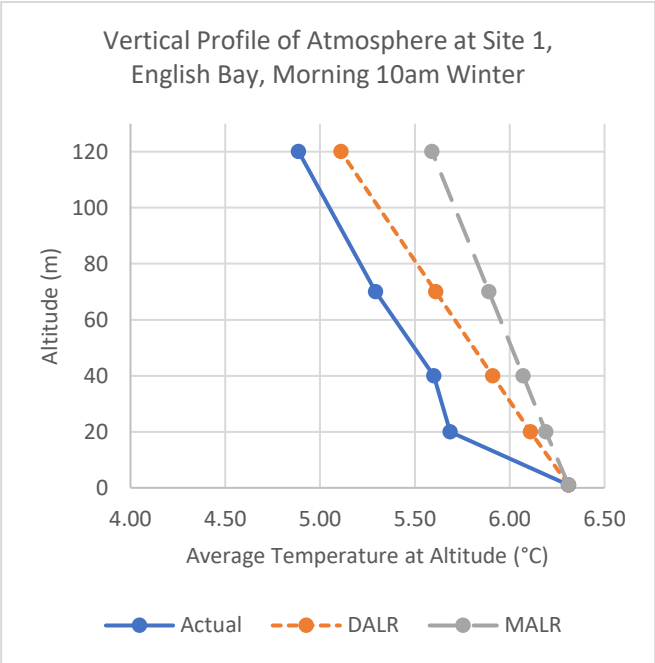
Vertical Profile of Atmosphere at Site 1, English Bay, Morning 10am Winter
Altitude (m)
120
100
80
60
40
20
0
4.00
4.50
5.00
5.50
6.00
6.50
Average Temperature at Altitude (°C)
Actual
DALR
MALR

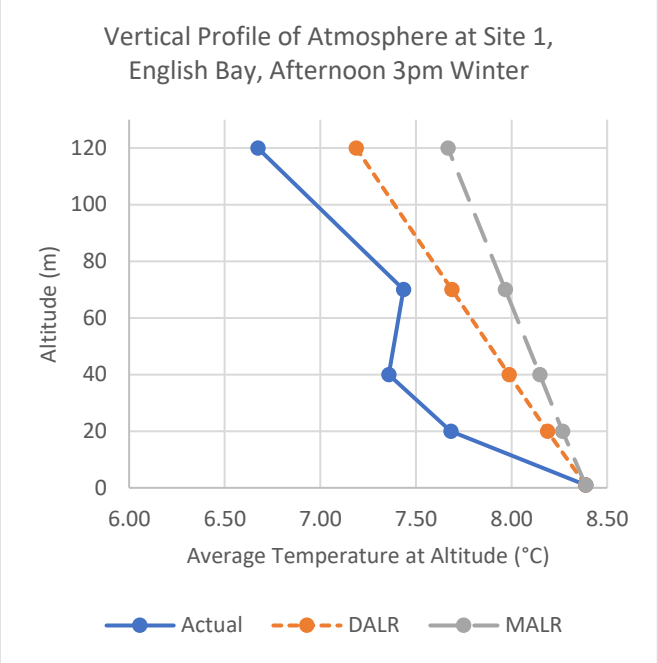
Vertical Profile of Atmosphere at Site 1, English Bay, Afternoon 3pm Winter
Altitude (m)
120
100
80
60
40
20
0
6.00
6.50
7.00
7.50
8.00
8.50
Average Temperature at Altitude (°C)
Actual
DALR
MALR

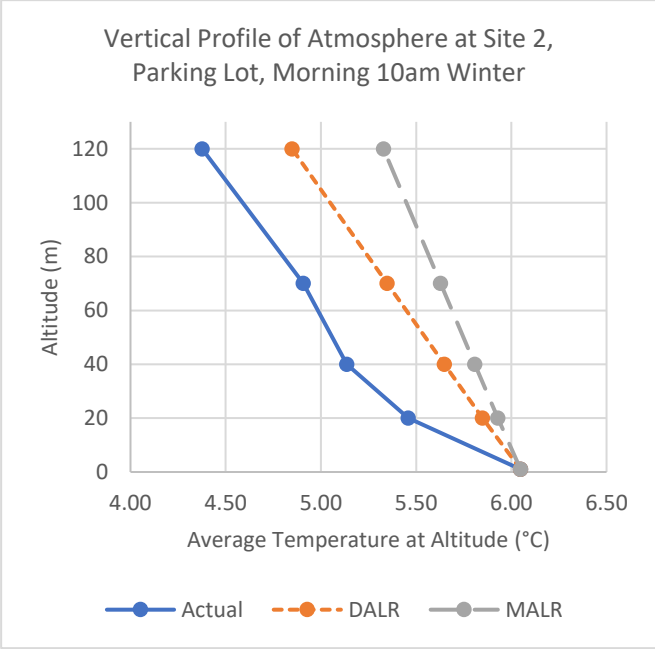
Vertical Profile of Atmosphere at Site 2, Parking Lot, Morning 10am Winter
Altitude (m)
120
100
80
60
40
20
0
4.00
4.50
5.00
5.50
6.00
6.50
Average Temperature at Altitude (°C)
Actual
DALR
MALR

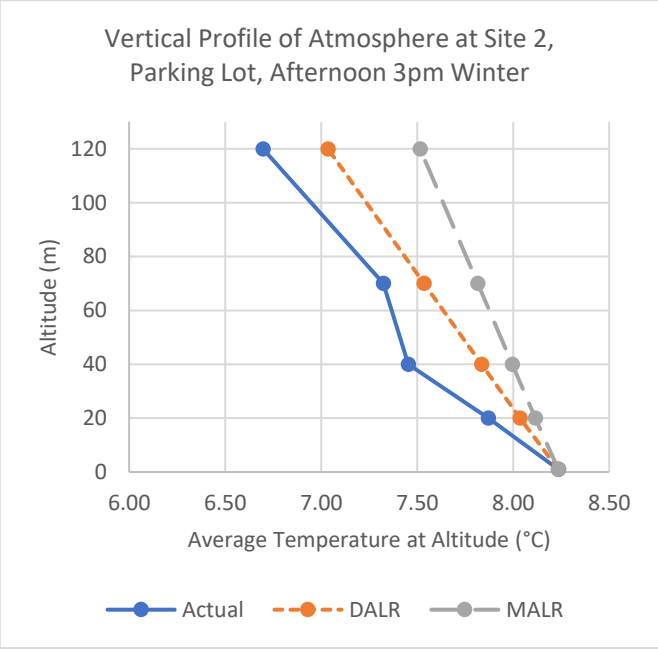
Vertical Profile of Atmosphere at Site 2, Parking Lot, Afternoon 3pm Winter
Altitude (m)
120
100
80
60
40
20
0
6.00
6.50
7.00
7.50
8.00
8.50
Average Temperature at Altitude (°C)
Actual
DALR
MALR

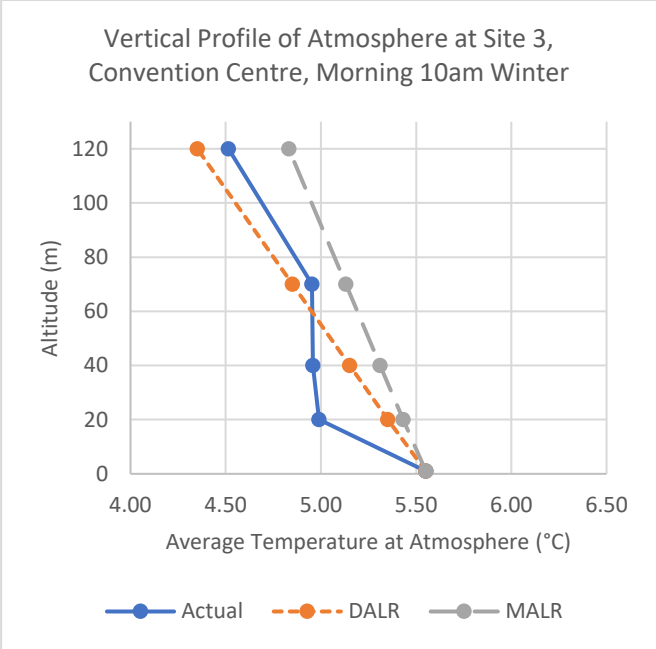
Vertical Profile of Atmosphere at Site 3, Convention Centre, Morning 10am Winter
Altitude (m)
120
100
80
60
40
20
0
4.00
4.50
5.00
5.50
6.00
6.50
Average Temperature at Atmosphere (°C)
Actual
DALR
MALR

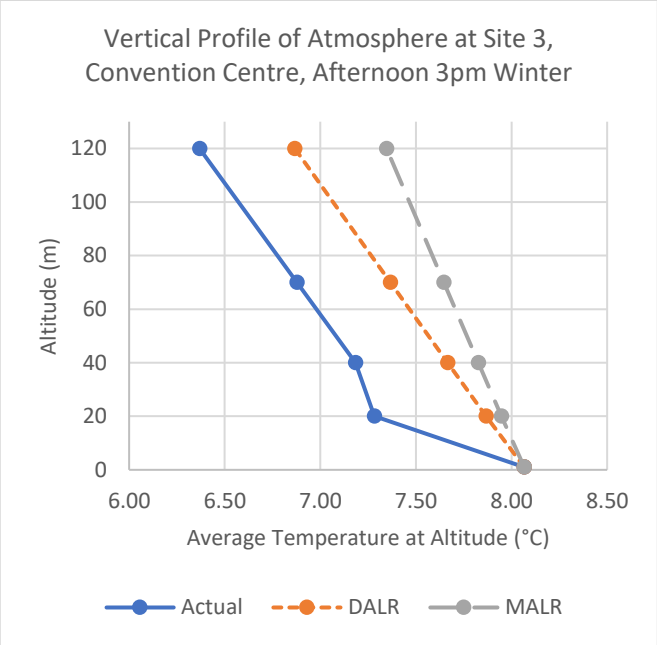
Vertical Profile of Atmosphere at Site 3, Convention Centre, Afternoon 3pm Winter
Altitude (m)
120
100
80
60
40
20
0
6.00
6.50
7.00
7.50
8.00
8.50
Average Temperature at Altitude (°C)
Actual
DALR
MALR

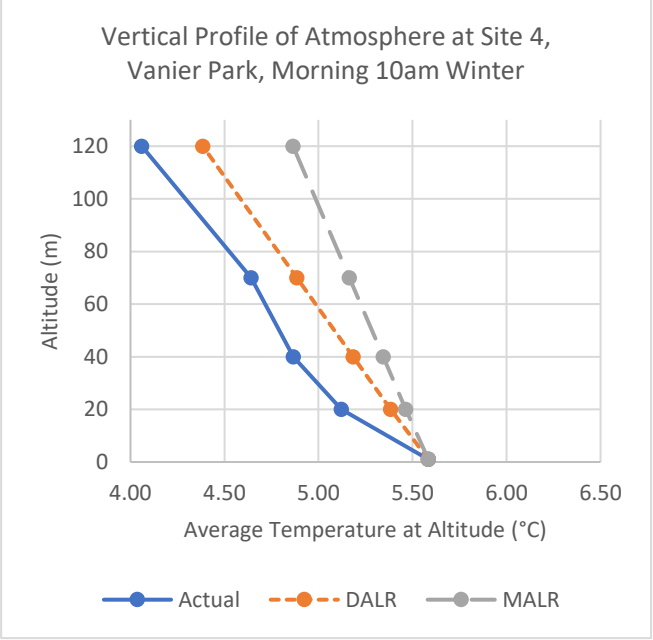
Vertical Profile of Atmosphere at Site 4, Vanier Park, Morning 10am Winter
Altitude (m)
120
100
80
60
40
20
0
4.00
4.50
5.00
5.50
6.00
6.50
Average Temperature at Altitude (°C)
Actual
DALR
MALR

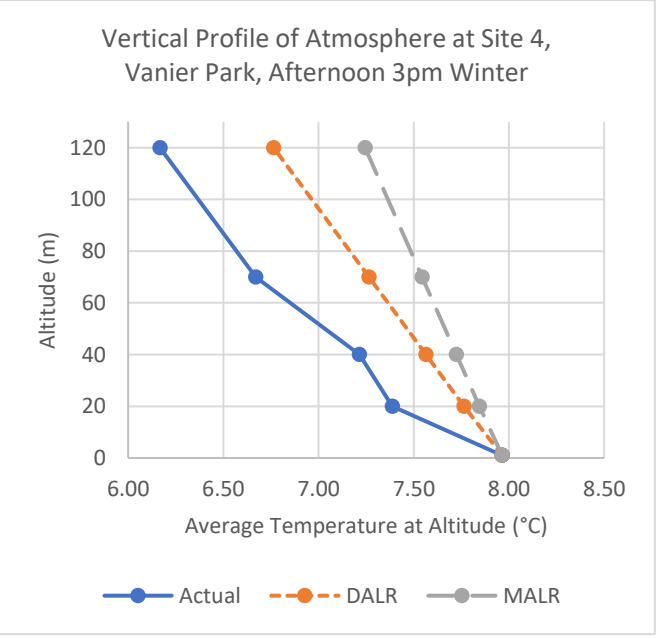
Vertical Profile of Atmosphere at Site 4, Vanier Park, Afternoon 3pm Winter
Altitude (m)
120
100
80
60
40
20
0
6.00
6.50
7.00
7.50
8.00
8.50
Average Temperature at Altitude (°C)
Actual
DALR
MALR